Classification and construction of interacting fractonic higher-order topological phases

Jian-Hao Zhang [1] Meng Cheng,[2,*] and Zhen Bi[1,†]

[1]*Department of Physics, The Pennsylvania State University, University Park, Pennsylvania 16802, USA*
[2]*Department of Physics, Yale University, New Haven, Connecticut 06511-8499, USA*

The notion of higher-order topological phases can have interesting generalizations to systems with subsystem symmetries that exhibit fractonic dynamics for charged excitations. In this work, we systematically study the higher-order topological phases protected by a combination of subsystem symmetries and ordinary global symmetries in two and three-dimensional interacting boson systems, with some interacting fermionic examples. In particular, we discover some important results, including (i) an Abelian subsystem symmetry group that does not allow for a nontrivial higher-order symmetry-protected topological phase in 2D without global symmetry. (ii) inhomogeneous subsystem symmetries do not allow for that either.

I. INTRODUCTION

Symmetry-protected topological (SPT) phases greatly expand our knowledge of quantum phases of matter beyond the conventional Landau symmetry-breaking paradigm [1–4]. Tremendous progress has been made over the past decade in classifying and characterizing SPT phases with internal and crystalline symmetries [5–15]. A common feature of SPT phases is that the boundary of an SPT phase is usually gapless due to symmetry protection. For instance, the celebrated $3d$ topological insulator hosts single massless Dirac cones protected by charge conservation and time reversal symmetry on its $2d$ surfaces. However, in contrast to the phenomenology of the ordinary topological insulator, recently a new class of SPT phases is shown to exist where symmetry-protected gapless modes only show up on certain low-dimensional submanifolds on the boundary while the majority of the boundary can be gapped without breaking the symmetry. These features defined a new class of SPT phases which is dubbed higher-order topological phases [16–20].

Higher-order topological phases turn out to be rather common in systems with crystalline symmetries. A great deal of weakly interacting higher-order topological insulators and superconductors has been established theoretically [21–33] and discovered experimentally [34–37] as well. For strongly interacting systems of fermions or bosons, one can also demonstrate the existence and study the properties of higher-order topological phases with methods such as the crystalline equivalence principle [26] and the block state constructions [38–43]. These studies bring us a complete picture of symmetry-protected topological phases with crystalline symmetries.

Coming from a rather orthogonal direction, a new type of symmetry, namely subsystem symmetry, is discovered

along the exploration of so-called fracton topological phases. Compared to ordinary global symmetry, subsystem symmetries are more closely intertwined with the underlying foliation [44–47] structure of space and only act on a rigid submanifold/leaf of the whole system. As the charges on each submanifold are conserved individually, single charge tunneling events are forbidden, which leads to fractonic behaviors [44–47]. Approximate subsystem symmetries have natural manifestations in certain physical systems. For instance, in twisted bilayer tungsten ditelluride systems, at a twist angle of 5°, experiments [48] exhibit exceptionally large transport anisotropy between two orthogonal in-plane directions, indicating vanishing single-particle tunneling in one direction. Another system with approximate subsystem symmetry is $3d$ kagome metal materials, Ni_3In as an example [49], where the single-particle tunnelings within xy plane are suppressed due to interference effects of atomic orbitals. Subsystem symmetry may also be an emergent symmetry at some quantum critical points [50].

A natural question is whether there are nontrivial SPT phases associated with subsystem symmetry. Indeed, previous works have shown the existence of subsystem symmetry-protected topological (SSPT) phases [51–66]. Examples of higher-order topological phases with subsystem symmetries are also discovered [67] but still lack a systematic understanding. In this work, we systematically study possible higher-order topological phases in strongly interacting bosonic systems protected by a combination of global and subsystem symmetries labeled by $G_g \times G_s$. We present a general scheme for classifying higher-order SSPT states, that applies to both bosonic and fermionic systems and work out the complete mathematical classification in the bosonic case. From the general classification, we establish a few interesting facts. For instance, for Abelian subsystem symmetry, there is no nontrivial two-foliated higher-order SSPT phase in (2+1)d systems without the aid of global symmetry. In addition, we prove that for inhomogeneous subsystem symmetries, there is no nontrivial higher-order SSPT phase. Besides the general

*m.cheng@yale.edu
†zjb5184@psu.edu

classification, we also explicitly construct models of such SSPT states in 2 and 3 spatial dimensions.

The rest of the paper is organized as follows. In Sec. II, we discuss the classifications and explicit model constructions of higher-order SPT phases with two-foliated subsystem symmetry. In particular, we prove that if G_g is trivial, there is no nontrivial higher-order SSPT phase in (2+1)D systems. Finally, in Sec. IV, we consider three-dimensional systems with the 3-foliation structure, including the classifications and explicit lattice model constructions. We will explicitly construct an exactly solvable lattice model of (3+1)D third-order SSPT phase with three-foliated $\mathbb{Z}_2 \times \mathbb{Z}_2$ subsystem symmetry. Furthermore, we will demonstrate that for arbitrary foliated inhomogeneous subsystem symmetries in any dimension, there is no nontrivial higher-order SSPT phase. In Sec. V, we summarize the main results of this paper and discuss further outlooks.

II. SECOND-ORDER SSPT PHASES WITH 2-FOLIATED SUBSYSTEM SYMMETRY

A foliation is a decomposition of a manifold into an infinite number of disjoint lower-dimensional submanifolds called leaves. By 2-foliation, we mean the physical system we consider can be decomposed into two orthogonal sets of disjoint codimension-1 submanifolds. And an independent conserved symmetry charge can be defined on each of these codimension-1 subsystems.

Before passing to the two-foliated systems, we want to mention that one-foliated systems cannot host any nontrivial higher-order SSPT phases even with global symmetry. The argument is presented in Appendix A.

In this section, we consider the system with two-foliated subsystem symmetries. We will assume that the symmetries are on-site, so the unitaries that implement the symmetry transformations are tensor products of unitaries acting on the Hilbert spaces of sites. We will generally consider the following two scenarios: (1) homogeneous subsystem symmetries where the two-foliated subsystem symmetries are built out of the same on-site symmetry transformations and (2) inhomogeneous subsystem symmetries where the symmetries in different directions act completely differently. As we will see, the two kinds of subsystem symmetries have significant physical differences, therefore, we discuss them separately. Schematically, we denote the subsystem symmetry group by G_s. In addition to the subsystem symmetries, we also consider an additional global symmetry, G_g, in the system. For simplicity, in this work, we consider the situation where the total symmetry is a direct product of G_s and G_g, although our formalism can be generalized to situations where the two groups have nontrivial central extensions straightforwardly.

A. General remarks

For a $(d + 1)$D lattice with a 2-foliation structure, for our purpose, it is convenient to think of the system as a square grid. Each site-(x, y) of the grid corresponds to a $(d - 2)$ system, whose Hilbert space is denoted by $\mathcal{H}_{xy}$. For $d > 2$ the $(d - 2)$D system itself may be extensive. The total Hilbert space is a tensor product $\mathcal{H} = \otimes_{x,y} \mathcal{H}_{xy}$. The two-foliated
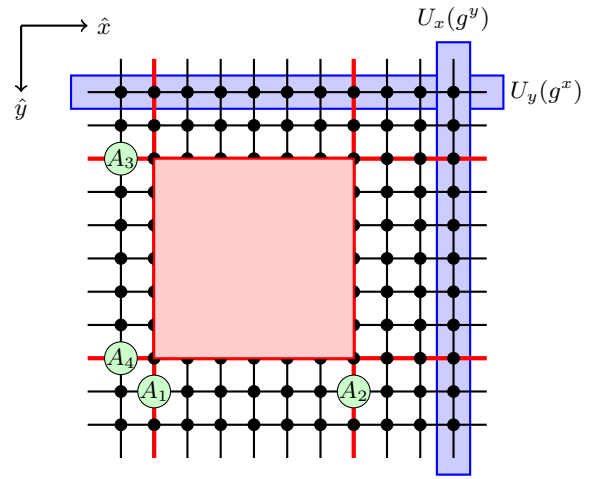

FIG. 1. Coupled-wire model with two-foliated subsystem symmetries $U_x(g^y)$ and $U_y(g^x)$. Blue strips depict subsystem symmetries, and $A_{1,2,3,4}$ depict the background gauge fields of corresponding subsystem symmetries marked by red solid lines.

homogeneous subsystem symmetries are defined as follows:

$$
\begin{aligned}
U_x(g) &= \prod_{y=-\infty}^{\infty} u_{xy}(g) \\
&\qquad\qquad\qquad , \quad g \in G_s, \qquad (1) \\
U_y(g) &= \prod_{x=-\infty}^{\infty} u_{xy}(g)
\end{aligned}
$$

where $u_{xy}(g)$ is an on-site unitary operator acting on the $(d - 2)$D system at site (x, y), and forms a faithful linear representation of the subsystem symmetry group G_s. The geometry of subsystem symmetries in $(2 + 1)$D systems is illustrated in Fig. 1.

So far G_s may be Abelian or non-Abelian. Suppose G_s is a non-Abelian group. For a given site (x, y), and $g_1, g_2 \in G_s$ we consider the following unitary:

$$
U_y(g_2^{-1}) U_x(g_1^{-1}) U_y(g_2) U_x(g_1) = u_{xy}(g_2^{-1} g_1^{-1} g_2 g_1). \qquad (2)
$$

This operator is nontrivial if and only if $g_2^{-1} g_1^{-1} g_2 g_1 \neq 1$. This commutator becomes a local symmetry of the site when this is the case. More generally, there is a local symmetry group $[G_s, G_s]$ on each site as the commutator of the subsystem symmetry G_s, and an effective Abelian subsystem symmetry $G_s' = G_s/[G_s, G_s]$ known as the Abelianization of G_s. Therefore it is sufficient to consider the Abelian subgroup of the non-Abelian subsystem symmetry [53].

There is another possible pattern of subsystem symmetry: the subsystem symmetries along the two directions are completely different, i.e., they have different group structures and have different actions. Suppose the subsystem symmetry along the horizontal/vertical direction is G_s^x/G_s^y, the two-foliated subsystem symmetries should be defined

as ($\forall x, y \in \mathbb{Z}$):

$$U_x(g^y) = \prod_{y=-\infty}^{\infty} u_{xy}^y(g^y)$$
$$U_y(g^x) = \prod_{x=-\infty}^{\infty} u_{xy}^x(g^x) \quad , \quad \begin{cases} g^x \in G_s^x \\ g^y \in G_s^y \end{cases}, \tag{3}$$

where $u_{xy}^y(g^y)/u_{xy}^x(g^x)$ is the linear representation of G_s^x/G_s^y on the site-(x, y), and $u_{xy}(g) = u_{xy}^y(g^y)u_{xy}^x(g^x)$ is the linear representation of $G_s^y \times G_s^x$ on the site-(x, y), $g = g^x g^y$.

We first consider systems with homogeneous subsystem symmetries and derive a complete classification.

B. Classification using boundary anomaly

Consider a system with finite extension in x and y, and infinite in the remaining directions. The boundary consists of two lines/planes parallel to x, and two parallel to y, with four (codimension-2) corners. By definition, the boundary is trivially gapped except at the corners. Each corner individually can be described by a theory in $(d - 2)$-dimensional space. The subsystem symmetries, when restricted to one corner, become internal global symmetries of the corner theory. For homogeneous subsystem symmetry, the two subsystem symmetries should have identical symmetry action in the corner theory, since the corner is where two submanifolds intersect. Label the four corners as BL, BR, TL, and TR (B for bottom, T for top, L for left, and R for right). The corresponding submanifolds passing through the four corners are labeled as 1, 2, 3, and 4, as illustrated in Fig. 1.

We now view this whole system as a $(d - 2)$-dimensional system, with a on-site symmetry group $G_s^{\times 4}$. Clearly, as a physical $(d - 2)$-dimensional system, the symmetry action of $G_s^{\times 4}$ must be free of any 't Hooft anomaly. This is the consistency condition that we will impose to classify the SSPT phases. But before going to the actual classification, first we review how to describe 't Hooft anomaly.

For a local quantum system in $(D + 1)$-dimensions (may be a lattice model or a continuum theory) with global unitary symmetry group G, the 't Hooft anomaly of G can be probed by coupling the system to a (flat) background G gauge field A. The anomaly is the fact that the system is not invariant under gauge transformations of the background gauge field A. Through the inflow mechanism, the anomaly can be uniquely associated with a $(D + 2)$-dimensional invertible theory (the background gauge field should also be extended to the $(D + 2)$-dimensional bulk). The topological response theory of the bulk to A will be denoted by $S[A]$, which should be a quantized topological term of the background gauge field A. For bosonic systems in $D \leqslant 2$ with unitary symmetry, the anomaly (and the associated SPT phases) can be fully classified by the group cohomology $\mathcal{H}^{D+2}(G, U(1))$. Namely, each anomaly class (or the SPT phase) is uniquely determined by a cohomology class $[\nu] \in \mathcal{H}^{D+2}(G, U(1))$, where ν is a representative group cocycle. Formally, the anomaly action can be written as

$$S_{\text{anomaly}}[A] = \int_{M_{D+2}} A^* \nu, \tag{4}$$

where we view the background gauge field A as a mapping from the space-time manifold M_{D+2} to the classifying space BG, and $A^* \nu$ is the pullback of $\mathcal{H}^d(BG, \mathbb{R}/\mathbb{Z})$.

In our case, since the symmetry group is $G_s^{\times 4}$, the background gauge fields can be written as (A_1, A_2, A_3, A_4), where the 1,2,3,4 indices indicate which subsystem the symmetry acts on, but we should keep in mind that in the $(d - 2)$-dimensional system they all become internal global symmetries. Since G_s is Abelian, we adopt the convention that the gauge field A_i's are all additive.

The structure of the system symmetry places more constraints on how the symmetries act on the corner theories. To give one example, consider the BL corner. By definition, $G_s^{(3)}$ and $G_s^{(4)}$ do not act on BL corner (so the theory is not coupled to A_3 and A_4), and $G_s^{(1)}$ and $G_s^{(2)}$ have identical symmetry actions. So when A_1 (or A_2) is turned on, the 't Hooft anomaly of the BL theory is captured by an action $S_{\text{BL}}[A_1]$ ($S_{\text{BL}}[A_2]$). However, when both A_1 and A_2 are turned on, the anomaly response of the BL corner theory becomes $S_{\text{BL}}[A_1 + A_2]$.

Now we consider the anomaly of $G_s^{(1)}$ alone. Equivalently, only A_1 is turned on. Both TL and BL corner theories are coupled to A_1, so the vanishing of the anomaly for $G_s^{(1)}$ implies

$$S_{\text{BL}}[A_1] + S_{\text{TL}}[A_1] = 0. \tag{5}$$

Similarly, we have

$$S_{\text{BR}}[A_2] + S_{\text{TR}}[A_2] = 0,$$
$$S_{\text{TL}}[A_3] + S_{\text{TR}}[A_3] = 0,$$
$$S_{\text{BL}}[A_4] + S_{\text{BR}}[A_4] = 0. \tag{6}$$

Thus the four response actions can all be related to, e.g., S_{BL}:

$$S_{\text{BR}}[A] = -S_{\text{BL}}[A],$$
$$S_{\text{TL}}[A] = -S_{\text{BL}}[A],$$
$$S_{\text{TR}}[A] = S_{\text{BL}}[A]. \tag{7}$$

Next we consider $G_s^{(1)} \times G_s^{(4)}$, i.e. turning on both A_1 and A_4, which intersect at the BL corner. The vanishing of the anomaly leads to

$$S_{\text{BL}}[A_1 + A_4] + S_{\text{TL}}[A_1] + S_{\text{BR}}[A_4] = 0. \tag{8}$$

Using the relations, we have

$$S_{\text{BL}}[A_1 + A_4] - S_{\text{BL}}[A_1] - S_{\text{BL}}[A_4] = 0. \tag{9}$$

It is important that the left-hand side should be viewed as the anomaly response for the symmetry group $G_s \times G_s$.

It is easy to see that considering other pairs of intersecting subsystem symmetries lead to the same mathematical condition as (9). Furthermore, once (9) is satisfied, the symmetry group $G_s^{\times 4}$ is indeed nonanomalous.

We now translate the condition (9) into a more concrete statement about the group cocycle. Suppose the anomaly action S_{BL} corresponds to a group cocycle $[\nu] \in \mathcal{H}^d(G_s, U(1))$. We introduce an "obstruction" map from $\mathcal{H}^d(G_s, U(1))$ to $\mathcal{H}^d(G_s \times G_s, U(1))$, as

$$f(\nu)((g_1, g_1'), \ldots, (g_d, g_d')) = \frac{\nu(g_1, \ldots, g_d)\nu(g_1', \ldots, g_d')}{\nu(g_1 g_1', \ldots, g_d g_d')}, \tag{10}$$

and the condition (9) is the statement that $[f(\nu)]$ is trivial in $\mathcal{H}^d(G_s \times G_s, U(1))$, which defines a subgroup of $\mathcal{H}^d(G_s, U(1))$.

We note that for $d = 2$, the corner theory is 0+1d and the only anomaly is the 't Hooft anomaly of a global symmetry, which essentially says the corner state transforms as a projective representation of the global symmetry. In $d = 3$, the corner theory is 1+1d, which may have a gravitational anomaly characterized by a chiral central charge c, which is always an integer multiple of 8 in bosonic systems. However, in that case, the gravitational anomaly and 't Hooft anomaly can be completely decoupled, and the vanishing of the gravitational anomaly requires

$$c_{BL} + c_{TL} + c_{BR} + c_{TR} = 0. \tag{11}$$

Then they can always be canceled by stacking layers of E_8 states on the four surfaces.

Next, we turn to the case with an additional global symmetry G_g. The story is similar but with a few twists. We will also need to turn on background gauge fields for the global symmetry, and the corner theory can have mixed anomalies between the global and the subsystem symmetries. We can assume that the corner theories do not carry any anomaly of the G_g symmetry alone, as they can be canceled by boundary reconstruction. This is analogous to the argument that we can ignore the gravitational anomaly.

Therefore the anomaly response for, e.g., the BL corner theory in the presence of both subsystem background gauge field A_s and A_g should take the following form:

$$S_{BL}[A_s] + S_{BL}[A_s, A_g]. \tag{12}$$

The first term is the subsystem symmetry anomaly, which we have already studied carefully. The second term represents the mixed anomaly. Namely, it is only nontrivial when both A_s and A_g are nontrivial.

Following the same anomaly vanishing argument, we find

$$S_{BR}[A_s, A_g] = -S_{BL}[A_s, A_g],$$
$$S_{TL}[A_s, A_g] = -S_{BL}[A_s, A_g],$$
$$S_{TR}[A_s, A_g] = S_{BL}[A_s, A_g]. \tag{13}$$

and

$$S_{BL}[A_s + A'_s, A_g] - S_{BL}[A_s, A_g] - S_{BL}[A'_s, A_g] = 0. \tag{14}$$

Let us turn it into an algebraic expression for the case of group-cohomology SPT phases. We assume that $S_{BL}[A_s, A_g]$ corresponds to a cocycle ν in $\mathcal{H}^d(G_s \times G_g, U(1))$. Denote the group elements of $G_s \times G_g$ by a pair (g, h) where $g \in G_s, h \in G_g$. Define the obstruction map from ν to $\mathcal{H}^d(G_s \times G_s \times G_g, U(1))$:

$$f(\nu)((g_1, g'_1, h_1), \ldots, (g_d, g'_d, h_d))$$
$$= \frac{\nu((g_1, h_1), \ldots, (g_d, h_d))\nu((g'_1, h_1), \ldots, (g'_d, h_d))}{\nu((g_1 g'_1, h_1), \ldots, (g_d g'_d, h_d))}. \tag{15}$$

Here we denote the elements of $G_s \times G_s \times G_g$ as (g, g', h).

The condition is then $f(\nu)$ corresponds to a trivial class in $\mathcal{H}^d(G_s \times G_s \times G_g, U(1))$.

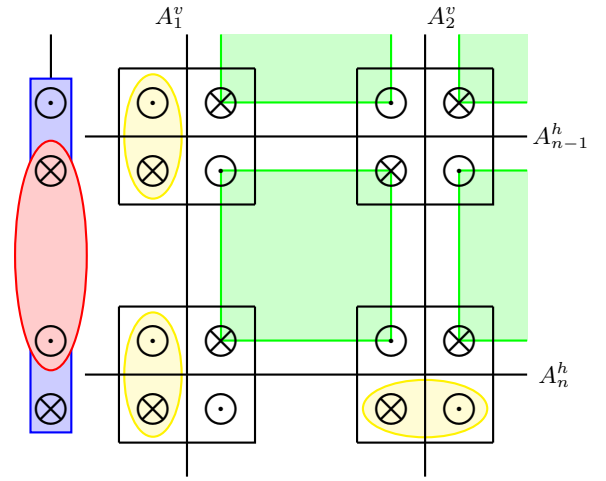FIG. 2. Illustration of the "coupled wire" construction. Each "⊗" represents a codimension-2 system with the given anomaly of G_s (e.g., a projective representation in $d = 2$, or a Luttinger liquid in $d = 3$), and each "⊙" represents a system with the opposite anomaly. Each square represents a "site," which has no anomaly for the G_s symmetry and thus can be realized by certain microscopic model. Green plaquettes represent the four-body interactions in bulk, and yellow ellipse for the on-site two-body coupling on the edge. $(A_1^v, A_2^v, A_{n-1}^h, A_n^h)$ are background gauge fields of subsystem symmetry G_s defined on different codimension-1 subsystems. On the left edge, a codimension-1 SSPT phase might be adhered to trivialize the bulk SSPT phase, each blue plate represents a site and each red ellipse represents a two-body inter-site coupling.

C. Microscopic constructions

Next, we demonstrate that all obstruction-vanishing anomalies can be realized in the corner theory of a bulk SSPT state, generalizing a "coupled wire" construction in Ref. [68].

For this, we can consider the following lattice construction. First we pick a $(d-2)$-dimensional symmetry-preserving gapless theory $\mathcal{T}$ with the given G_s anomaly class $S[A]$. For $d = 2$, it is a projective representation. For $d = 3$, one can choose a (1+1)d CFT with the given anomaly. Denote by $\overline{\mathcal{T}}$ the theory with the opposite anomaly (e.g., complex conjugating $\mathcal{T}$). Given a square grid as shown in Fig. 2, in each unit cell we arrange a $(d-2)$-dimensional theory $\mathcal{T}_{BL} \otimes \overline{\mathcal{T}}_{TL} \otimes \overline{\mathcal{T}}_{BR} \otimes \mathcal{T}_{TR}$. Within each unit cell, the symmetry G_s acts diagonally on the four theories. By construction, the unit cell has no G_s anomaly, so it should be possible to realize the theory in a physical $(d-2)$ system with on-site G_s symmetry.

Now we consider the whole grid. The subsystem symmetry is defined in the standard way. To construct the SSPT state, we turn on interactions at each square plaquette, coupling the four neighboring unit cells indicated by the green area in Fig. 2. Note that the coupling only involves one of the $\mathcal{T}$ or $\overline{\mathcal{T}}$ theory from each of the four unit cells. We require that the four theories involved in the plaquette interaction can be gapped out while preserving the subsystem symmetries. In order to do this, the subsystem symmetries acting on this green plaquette must be nonanomalous, which is precisely the condition previously in (9). In fact, it is believed that anomaly

vanishing is both sufficient and necessary in order to find a trivially gapped ground state [69]. So there should exist such an interaction.

Once the appropriate interactions are turned on and drive the bulk into a fully gapped state, there still exist nontrivial boundary modes. We assume that the system is terminated with "smooth" boundaries, as illustrated in Fig. 2. For each unit cell on the smooth edge, there are two dangling theories that are not included in the bulk plaquette interactions, with opposite anomalies (see Fig. 2). Hence we can simply introduce a coupling (see yellow ellipse in Fig. 2) between them preserving the subsystem symmetries to gap them out and obtain a fully gapped boundary. However, for the unit cell at the corner, there are three dangling theories that are not included in the bulk plaquette interactions, and two of them can be gapped by the above boundary couplings, leaving a dangling corner/hinge theory that carries the desired anomaly. Therefore this lattice construction gives a symmetric gapped bulk state with symmetric gapped edges but anomalous corner modes.

III. EXAMPLES

A. 2D systems with only subsystem symmetry

In this section, we prove the following. *There is no nontrivial two-foliated higher-order SSPT phase in (2+1)D without global symmetry.*

Let us think about abelian subsystem symmetry. It is well-known that any finite Abelian group can be written as a product of several cyclic groups:

$$G_s = \prod_{i=1}^{N} \mathbb{Z}_{n_i}, \; n_i \in \mathbb{Z}. \tag{16}$$

A group element $a \in G_s$ can be expressed as

$$a = (a_1, a_2, \cdots, a_N), \; a_{n_i} \in \mathbb{Z}_{n_i}. \tag{17}$$

The general expression of 2-cocycles in $\mathcal{H}^2[G_s, \mathrm{U}(1)]$ is

$$v_2(a, b) = \exp \left\{ 2\pi i \sum_{i<j} \frac{p_{ij}}{n_{ij}} a_i b_j \right\}, \tag{18}$$

where $p_{ij} \in \mathbb{Z}$ and $n_{ij} \in \mathbb{Z}$ is the greatest common divisor (GCD) of n_i and n_j. Substitute this explicit 2-cocycle into the obstruction-free condition (9), we conclude that an obstruction-free 2-cocycle corresponding to a nontrivial (2+1)D higher-order SSPT phase requires the following expression to be a 2-coboundary of the G_s^2 group:

$$v_2'[(a, a'), (b, b')] = \exp \left\{ 2\pi i \sum_{i<j} \frac{p_{ij}}{n_{ij}} (a_i b_j' + a_i' b_j) \right\}, \tag{19}$$

where a group element of G_s^2 is expressed as (a, a'), $a, a' \in G_s$. To determine if the 2-cocycle (19) is a nontrivial 2-cocycle in $\mathcal{H}^2[G_s^2, \mathrm{U}(1)]$, we should justify that v_2' is not commute for some (a, a') and $(b, b') \in G_s^2$ as

$$v_2'[(a, a'), (b, b')] \neq v_2'[(b, b'), (a, a')]. \tag{20}$$

With the explicit form of 2-cocycle in Eq. (19), we have

$$v_2'[(b, b'), (a, a')] = \exp \left\{ 2\pi i \sum_{i<j} \frac{p_{ij}}{n_{ij}} (b_i a_j' + b_i' a_j) \right\},$$

which is not equal to Eq. (19) if not all $n_{ij} = 1$ for $\forall i, j$. As a consequence, we have proved that all 2-cocycles like Eq. (18) are obstructed, and there is no nontrivial two-foliated higher-order SSPT phase in (2+1)D systems without global symmetry, for all Abelian subsystem symmetries.

Furthermore, we have argued that for non-Abelian subsystem symmetry, it is sufficient to consider its Abelian subgroup $G_s' = G_s/[G_s, G_s]$, hence even for non-Abelian subsystem symmetry, there is no (2+1)D higher-order SSPT phase without the aids of some proper global symmetry.

B. 2D bosonic SSPT with both subsystem and global symmetries

The mixed anomaly between G_s and G_g in this case is classified by $\omega \in \mathcal{H}^1[G_s, \mathcal{H}^1[G_g, \mathrm{U}(1)]]$. Let us write the 2-cocycle down explicitly. ω can be viewed as a group homomorphism between G_s and $\mathcal{H}^1(G_g, \mathrm{U}(1))$, the latter is the group of one-dimensional representations on G_g. Thus the corresponding 2-cocycle can be written as

$$v((g_s, g_g), (h_s, h_g)) = [\omega(g_s)](h_g). \tag{21}$$

Here $\omega(g_s)$ gives a one-dimensional representation of G_g and evaluating it on h_g yields the 2-cocycle. The obstruction is given by

$$
\begin{aligned}
f(v)&((g_s, g_s', g_g), (h_s, h_s', h_g)) \\
&= \frac{v((g_s, g_g), (h_s, h_g))v((g_s', g_g), (h_s', h_g))}{v((g_s g_s', g_g), (h_s h_s', h_g))} \\
&= \frac{[\omega(g_s)](h_g)[\omega(g_s')](h_g)}{[\omega(g_s g_s')](h_g)} \\
&= \left[\frac{\omega(g_s)\omega(g_s')}{\omega(g_s g_s')} \right](h_g) = 1. \tag{22}
\end{aligned}
$$

Thus the obstruction vanishes automatically.

Here we present an example to make our construction and classification of SSPT phases more concrete. $G_s = \mathbb{Z}_2$ and $G_g = \mathbb{Z}_2$. There is a two-dimensional projective representation protected by both G_s and G_g. We will construct a 2D SSPT phase with the projective representation as the corner mode.

We use the lattice construction in Fig. 2, where each circle is a spin-1/2 degree of freedom. The subsystem symmetry is generated by products of $\sigma_{\mathbf{R}}^z$ along rows and columns, and the global $\mathbb{Z}_2$ symmetry is generated by $\prod_{\mathbf{R}} \sigma_{\mathbf{R}}^x$. The green plate in Fig. 2 now includes four spin-1/2's, and we can introduce a ring-exchange coupling in each plaquette:

$$H_r = -\sum_{\mathbf{R}} \sigma_{\mathbf{R}}^+ \sigma_{\mathbf{R}+\hat{x}}^- \sigma_{\mathbf{R}+\hat{x}+\hat{y}}^+ \sigma_{\mathbf{R}+\hat{y}}^- + \mathrm{H.c.}, \tag{23}$$

where $\sigma^\pm = \sigma^x + i\sigma^y$, $\mathbf{R}$ labels the lattice sites and $\hat{x}/\hat{y}$ represents the unit vector along the x/y direction.

This Hamiltonian has the unique ground state on the lattice with periodic boundary condition (PBC) [51]:

$$|\Psi_0\rangle = \prod_P (|\downarrow_{BL}, \uparrow_{TL}, \uparrow_{BR}, \downarrow_{TR}\rangle_P$$
$$+ |\uparrow_{BL}, \downarrow_{TL}, \downarrow_{BR}, \uparrow_{TR}\rangle_P), \quad (24)$$

where the subscript P depicts different plaquettes. For sites on the edge and corner, we turn on a Heisenberg interaction $\sigma \cdot \sigma'$ in each yellow ellipse in Fig. 2, which can gap out a pair of spin-1/2 degrees of freedom on all edge sites, except one at the corner. As the consequence, there is only one dangling spin-1/2 degree of freedom at each corner of the lattice that remains gapless.

We notice that the Hamiltonian in fact has more symmetries. For example, the subsystem symmetry group can be enlarged to U(1), generated by the total σ^z along each row and column.

C. 3D bosonic SSPT with $G_s = \mathbb{Z}_2$

Let us work out the classification of 2nd-order SSPT phases in 3D for $G_s = \mathbb{Z}_2$ and no global symmetry. Since $\mathcal{H}^3(\mathbb{Z}_2, U(1)) = \mathbb{Z}_2$, we just need to check whether the obstruction vanishes for the nontrivial class. Denote $\mathbb{Z}_2 = \{1, g\}$, and the nontrivial class is

$$\nu(g, g, g) = -1. \quad (25)$$

The obstruction mapping gives a $\mathcal{H}^3$ class $f(\nu)$ for the group $\mathbb{Z}_2 \times \mathbb{Z}_2$. We will check the three invariants of the cohomology class:

$$f(\nu)((g, 1), (g, 1), (g, 1)) = 1,$$
$$f(\nu)((1, g), (1, g), (1, g)) = 1,$$
$$f(\nu)((g, g), (g, g), (g, g)) = \nu(g, g, g)^2 = 1. \quad (26)$$

Therefore $f(\nu)$ belongs to the trivial class and the obstruction vanishes. We conclude that the classification is given by $\mathbb{Z}_2$.

Below we provide an explicit construction of the SSPT phase using a coupled wire model. The $(1+1)$D system as the building block of the coupled-wire model can only be the edge theory of the $(2+1)$D Levin-Gu model [70], which can be represented in terms of a two-component Luttinger theory:

$$\mathcal{L}_0 = \frac{1}{2\pi} \partial_x \phi_1 \partial_\tau \phi_2 + \frac{1}{4\pi} \sum_{\alpha,\beta=1,2} \partial_x \phi_\alpha V_{\alpha\beta} \partial_x \phi_\beta. \quad (27)$$

The $\mathbb{Z}_2$ symmetry is generated by the following action:

$$\phi_1 \to \phi_1 + \pi, \quad \phi_2 \to \phi_2 + \pi. \quad (28)$$

Consider the green plaquette in Fig. 2 including four Luttinger liquids (27), the overall Lagrangian of these four Luttinger liquids is

$$\mathcal{L} = \frac{1}{4\pi} \partial_x \Phi^T K \partial_\tau \Phi + \frac{1}{4\pi} \partial_x \Phi^T V \partial_x \Phi. \quad (29)$$

where $\Phi = (\phi_1, \ldots, \phi_8)^T$ is the eight-component boson field, $K = (\sigma^x)^{\oplus 4}$ is the K matrix. There are four $\mathbb{Z}_2$ subsystem symmetries $\mathbb{Z}_2^j$ ($j = 1, 2, 3, 4$) defined in different directions. Their actions on the bosonic fields, following from, all take

the form $\Phi \to \Phi + \delta\Phi$, where

$$\delta\Phi^{\mathbb{Z}_2^1} = \pi(1, 1, 1, 1, 0, 0, 0, 0)^T,$$
$$\delta\Phi^{\mathbb{Z}_2^2} = \pi(0, 0, 0, 0, 1, 1, 1, 1)^T,$$
$$\delta\Phi^{\mathbb{Z}_2^3} = \pi(1, 1, 0, 0, 0, 0, 1, 1)^T,$$
$$\delta\Phi^{\mathbb{Z}_2^4} = \pi(0, 0, 1, 1, 1, 1, 0, 0)^T. \quad (30)$$

We then need to construct gapping terms that gap out the edge without breaking symmetry, neither explicitly nor spontaneously. Consider backscattering terms of the form:

$$U = U_0 \sum_k \cos\left(l_k^T K \Phi\right). \quad (31)$$

Since there are eight bosonic fields, four independent, mutually commuting gapping terms are needed to completely gap out the edge. More precisely, the vectors $\{l_k\}$ must satisfy the "null-vector" conditions [71] for $\forall i, j$:

$$l_i^T K l_j = 0. \quad (32)$$

In addition, the interactions must preserve the $\mathbb{Z}_2$ symmetries, which means for each i

$$l_i^T K \delta\Phi = 0, \quad (33)$$

for each of the $\delta\Phi$ in Eq. (30).

We find the following vectors satisfy all the requirements:

$$l_1^T = (1, 0, 1, 0, 1, 0, 1, 0),$$
$$l_2^T = (0, 1, 0, -1, 0, -1, 0, 1),$$
$$l_3^T = (1, 0, 0, -1, 1, 0, 0, 1),$$
$$l_4^T = (0, 1, -1, 0, 0, -1, -1, 0). \quad (34)$$

Furthermore, in order to obtain a fully-gapped bulk state, we should avoid spontaneous symmetry breaking, which would lead to ground-state degeneracy in each plaquette. Following the method described in [5,72], we confirm that the gapping terms leave a unique ground state, thus no spontaneous symmetry breaking. To summarize, we find that the Higgs terms (34) provide a fully-gapped bulk state. We note that all these Higgs terms are four-body interactions, hence the fully gapped bulk state does not have any layered structure.

For the sites on the $(2+1)$D surface, there are two Luttinger liquids (27) that are not included in the bulk interactions (see yellow ellipses in Fig. 2). The total Lagrangian of these two Luttinger liquids is

$$\mathcal{L}_s = \left(\partial_x \phi_s^T\right) \frac{K^s}{4\pi} (\partial_\tau \phi_s) + \left(\partial_x \phi_s^T\right) \frac{V^s}{4\pi} (\partial_x \phi_s), \quad (35)$$

where $\phi_s^T = (\phi_1, \phi_2, \phi_3, \phi_4)$ is the 4-component chiral boson field, $K^s = (\sigma^x)^{\oplus 2}$ is the K-matrix. The on-site $\mathbb{Z}_2$ symmetry is defined as:

$$W^{\mathbb{Z}_2} = \mathbb{1}_{4\times 4}, \quad \delta\phi = \pi(1, 1, 1, 1)^T. \quad (36)$$

We can simply gap out these two Luttinger liquids by two on-site Higgs terms (31) with the following null-vectors:

$$l_1^T = (1, 0, 1, 0),$$
$$l_2^T = (0, 1, 0, -1). \quad (37)$$

And a fully gapped $(2+1)$D surface state is obtained.

For the sites at the hinge of the system, there are three dangling (1+1)D Luttinger liquids that are not included in the bulk interactions, where two of them can be gapped by the Higgs term like Eq. (37). Hence the remaining gapless Luttinger liquid with the Lagrangian (27) will be the hinge mode of the constructed coupled-wire model.

We should further investigate the stability of the hinge mode in order to make sure that the coupled-wire model we have constructed characterizes a nontrivial (3+1)D SSPT phase. Consider a potential (2+1)D SSPT phase protected by G_s adhering at the left surface of the system (see Fig. 2) as an assembly of (1+1)D Luttinger liquids, each site includes two Luttinger liquids (see blue rectangles in Fig. 2), each of them has the Lagrangian (27). On the one hand, they can be gapped on the on-site stage, by introducing the Higgs terms corresponding to the null-vectors in Eq. (37). On the other hand, we prove that the inter-site coupling of the Luttinger liquids is prohibited by horizontal subsystem symmetry: consider two Luttinger liquids included in a red ellipse in Fig. 2, there are two subsystem symmetries $\mathbb{Z}_2^1$ and $\mathbb{Z}_2^2$ defined on different vertical coordinates along the horizontal direction:

$$
\begin{aligned}
\delta\phi^{\mathbb{Z}_2^1} &= \pi(1, 1, 0, 0)^{\mathrm{T}}, \\
\delta\phi^{\mathbb{Z}_2^2} &= \pi(0, 0, 1, 1)^{\mathrm{T}}.
\end{aligned}
\tag{38}
$$

We can rigorously prove that these two Luttinger liquids in a red ellipse cannot be gapped [73]. Thus the (1+1)D hinge mode as the edge theory of the (2+1)D Levin-Gu state is robust against adhering a (2+1)D SSPT phase to the edge of the system, and we have constructed a nontrivial two-foliated $\mathbb{Z}_2$ SSPT phase.

D. 3D bosonic SSPT with $G_s = \mathbb{Z}_2$ and $G_g = \mathbb{Z}_2^T$

In this section, we explicit construct the coupled-wire model of (3+1)D second-order SSPT with two-foliated subsystem symmetry $\mathbb{Z}_2$ and a global time-reversal symmetry $\mathbb{Z}_2^T$. The Luttinger liquid we work on as the building block carries the mixed anomaly of $\mathbb{Z}_2$ and $\mathbb{Z}_2^T$, which is classified by $\mathcal{H}^1(\mathbb{Z}_2, \mathcal{H}^2[\mathbb{Z}_2^T, U_T(1)])$. The two-component Luttinger liquid takes the form of Eq. (27), with the following symmetry properties

$$
\begin{aligned}
\mathbb{Z}_2 &: \phi_1 \mapsto \phi_1 + \pi, \ \phi_2 \mapsto \phi_2, \\
\mathbb{Z}_2^T &: \phi_1 \mapsto \phi_1, \ \phi_2 \mapsto -\phi_2 + \pi.
\end{aligned}
\tag{39}
$$

Again consider the green block in Fig. 2 including four Luttinger liquids (27), the overall Lagrangian takes the form of (29). There are four $\mathbb{Z}_2$ subsystem symmetries $\mathbb{Z}_2^j$ ($j = 1, 2, 3, 4$) defined in different directions. These $\mathbb{Z}_2$ actions take the form of $\Phi \mapsto \Phi + \delta\Phi$, where

$$
\begin{aligned}
\delta\Phi^{\mathbb{Z}_2^1} &= \pi(1, 0, 1, 0, 0, 0, 0, 0)^{\mathrm{T}}, \\
\delta\Phi^{\mathbb{Z}_2^2} &= \pi(0, 0, 0, 0, 1, 0, 1, 0)^{\mathrm{T}}, \\
\delta\Phi^{\mathbb{Z}_2^3} &= \pi(1, 0, 0, 0, 0, 0, 1, 0)^{\mathrm{T}}, \\
\delta\Phi^{\mathbb{Z}_2^4} &= \pi(0, 0, 1, 0, 1, 0, 0, 0)^{\mathrm{T}},
\end{aligned}
\tag{40}
$$

and the global time-reversal symmetry acts as $\Phi \mapsto W^{\mathcal{T}}\Phi + \delta\Phi^{\mathcal{T}}$, where $W^{\mathcal{T}} = (\sigma^z)^{\oplus 4}$ and $\delta\Phi^{\mathcal{T}} = \pi(0, 1, 0, 1, 0, 1, 0, 1)^{\mathrm{T}}$. In order to gap out all eight

components of the boson fields, we need at least four independent Higgs terms (31) with four null-vectors $\{l_k\}$. We find that the following null-vectors satisfy all conditions:

$$
\begin{aligned}
l_1^{\mathrm{T}} &= (1, 0, 0, 0, 1, 0, 0, 0), \\
l_2^{\mathrm{T}} &= (1, 0, 1, 0, 0, 0, 0, 0), \\
l_3^{\mathrm{T}} &= (0, 0, 0, 0, 1, 0, 1, 0), \\
l_4^{\mathrm{T}} &= (0, 1, 0, 1, 0, 1, 0, 1),
\end{aligned}
\tag{41}
$$

which avoids spontaneous symmetry breaking.

For the sites on the (2+1)D surface, there are two Luttinger liquids (27) that are not included in the bulk interactions (see yellow ellipses in Fig. 2). The Lagrangian of these two Luttinger liquids takes the form of Eq. (35). The on-site $\mathbb{Z}_2 \times \mathbb{Z}_2^T$ symmetry is defined as

$$
\begin{aligned}
W^{\mathbb{Z}_2} &= \mathbb{1}_{4\times 4}, \ \delta\phi^{\mathbb{Z}_2} = \pi(1, 0, 1, 0)^{\mathrm{T}}, \\
W^{\mathbb{Z}_2^T} &= (\sigma^z)^{\oplus 2}, \ \delta\phi^{\mathbb{Z}_2} = \pi(0, 1, 0, 1)^{\mathrm{T}}.
\end{aligned}
\tag{42}
$$

By introducing the following two Higgs terms, we can simply gap out these Luttinger liquids and obtain a fully-gapped (2+1)D surface state

$$
\begin{aligned}
l_1^{\mathrm{T}} &= (1, 0, 1, 0), \\
l_2^{\mathrm{T}} &= (0, 1, 0, 1).
\end{aligned}
\tag{43}
$$

For the sites at the hinge which include three dangling Luttinger liquids (27), the above two of them can simply be gapped out by surface Higgs terms. Therefore the remaining gapless Luttinger liquid should be the second-order hinge mode of the (3+1)D SSPT phase with two-foliated $\mathbb{Z}_2$ subsystem symmetry and a global time-reversal symmetry $\mathbb{Z}_2^T$ who carries their mixed anomaly.

E. 3D fermionic SSPT with $G_s = \mathbb{Z}_2^f$ and $G_g = \mathbb{Z}_2$

Our arguments can also be generalized to interacting fermionic systems. We demonstrate this generalization by an example with $G_s = \mathbb{Z}_2^f$ and $G_g = \mathbb{Z}_2$. The (1+1)D Luttinger liquid as the building block of the coupled-wire model is

$$
\mathcal{L}_0 = \frac{1}{4\pi}\partial_x\phi^{\mathrm{T}}\sigma^z\partial_t\phi + \frac{1}{4\pi}\sum_{\alpha,\beta=1,2}\partial_x\phi_\alpha V_{\alpha\beta}\partial_x\phi_\beta.
\tag{44}
$$

The $\mathbb{Z}_2$ symmetry is defined as

$$
\phi_1 \mapsto \phi_1, \ \phi_2 \mapsto -\phi_2
\tag{45}
$$

and $\mathbb{Z}_2^f$ fermion parity as

$$
\phi_1 \mapsto \phi_1 + \pi, \ \phi_2 \mapsto \phi_2 + \pi.
\tag{46}
$$

Repeatedly consider the green plaquette in Fig. 2 composed of four Luttinger liquids (44), forming the overall Lagrangian as

$$
\mathcal{L} = \frac{1}{4\pi}\partial_x\Phi^{\mathrm{T}}K\partial_\tau\Phi + \frac{1}{4\pi}\partial_x\Phi^{\mathrm{T}}V\partial_x\Phi,
\tag{47}
$$

where $\Phi = (\phi_1, \cdots, \phi_8)^{\mathrm{T}}$ is the eight-component boson field, $K = (\sigma_z)^{\oplus 4}$ is the K matrix. There are four $\mathbb{Z}_2^f$ subsystem symmetries $\mathbb{Z}_{2,j}^f$ ($j = 1, 2, 3, 4$) in different directions with

an additional $\mathbb{Z}_2$ global symmetry. The fermion parities act on the boson fields have the form $\Phi \mapsto \Phi + \delta\Phi$, where

$$\delta\Phi^{\mathbb{Z}_{2,1}^f} = \pi(1, 1, 1, 1, 0, 0, 0, 0)^T,$$

$$\delta\Phi^{\mathbb{Z}_{2,2}^f} = \pi(0, 0, 0, 0, 1, 1, 1, 1)^T,$$

$$\delta\Phi^{\mathbb{Z}_{2,3}^f} = \pi(1, 1, 0, 0, 0, 0, 1, 1)^T,$$

$$\delta\Phi^{\mathbb{Z}_{2,4}^f} = \pi(0, 0, 1, 1, 1, 1, 0, 0)^T \tag{48}$$

and the global $\mathbb{Z}_2$ symmetry action takes the form $\Phi \mapsto W\Phi$, where $W = (\sigma^z)^{\oplus 4}$. In order to gap out all these boson fields, we need to find four independent Higgs terms like Eq. (31) while vectors $\{l_k\}$ ($k = 1, 2, 3, 4$) must be null-vectors [71]. We find the following null-vectors:

$$l_1^T = (1, 0, 0, 1, 1, 0, 0, 1),$$

$$l_2^T = (0, 1, 1, 0, 0, 1, 1, 0),$$

$$l_3^T = (1, 1, 1, 1, 0, 0, 0, 0),$$

$$l_4^T = (1, 1, 0, 0, 1, 1, 0, 0), \tag{49}$$

and the corresponding gapping terms avoid spontaneous symmetry breaking.

For the sites on the (2+1)D surface, there are two Luttinger liquids (44), as illustrated by yellow ellipses in Fig. 2. These two Luttinger liquids form the following Lagrangian:

$$\mathcal{L}_s = \partial_x \phi_s^T \frac{K^s}{4\pi} \partial_t \phi_s + \partial_x \phi_s^T \frac{V^s}{4\pi} \partial_x \phi_s, \tag{50}$$

where $\phi_s^T = (\phi_1, \cdots, \phi_4)$ is the four-component boson field and $K^s = (\sigma^z)^{\oplus 2}$ is the K-matrix. The on-site $\mathbb{Z}_2 \times \mathbb{Z}_2^f$ is defined as

$$W^{\mathbb{Z}_2} = (\sigma^z)^{\oplus 2}, \quad \delta\phi^{\mathbb{Z}_2} = 0,$$

$$W^{\mathbb{Z}_2^f} = \mathbb{1}_{4\times 4}, \quad \delta\phi^{\mathbb{Z}_2} = \pi(1, 1, 1, 1). \tag{51}$$

These boson fields can simply be gapped out through two Higgs terms (31) with the following null-vectors to obtain a fully gapped (2+1)D surface state:

$$l_1^T = (1, 0, 0, 1),$$

$$l_2^T = (0, 1, 1, 0). \tag{52}$$

Finally, for the sites at the hinge of the system, there are three dangling (1+1)D Luttinger liquids (44), where two of them can be gapped by the surface Higgs terms. Therefore the remaining gapless Luttinger liquid will be the hinge mode of the constructed coupled wire model of (3+1)D SSPT phase with two-foliated $\mathbb{Z}_2^f$ fermion parities and a global $\mathbb{Z}_2$ symmetry.

IV. THIRD-ORDER SSPT PHASES IN 3D SYSTEMS

Next, we consider the 3d systems with three-foliated subsystem symmetries and demonstrate the resulting third-order SSPT phases.

A. Classification using boundary anomaly

We consider systems with homogeneous subsystem symmetries and derive a complete classification. For (3+1)D
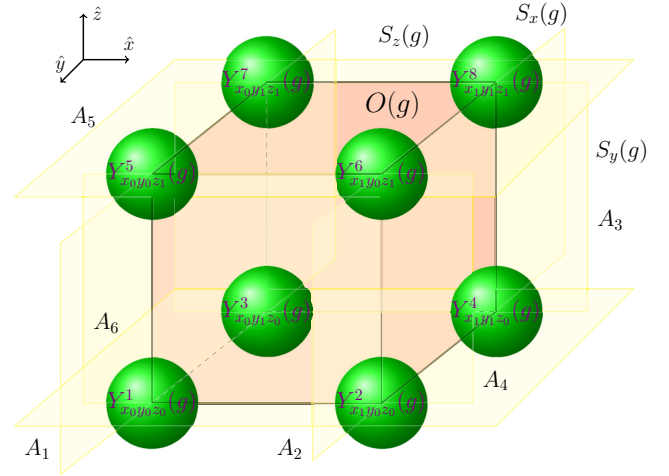

FIG. 3. (3+1)D lattice model with three-foliated subsystem symmetries $U_x(g)$, $U_y(g)$, and $U_z(g)$. Yellow plates depict subsystem symmetries, and the truncated symmetry operator $O(g)$ is depicted by a red cubic that only creates 0D excitations at the corners as illustrated by green balls. A_j ($j = 1, 2, 3, 4, 5, 6$) depicts the background gauge fields of corresponding subsystem symmetries.

systems with three-foliated homogeneous subsystem symmetries, there is an on-site symmetry group G_s on each site (x, y, z) acting as a unitary representation $u_{xyz}(g)$ on the local Hilbert space $\mathcal{H}_{xyz}$, while the total Hilbert space is $\mathcal{H} = \otimes_{x,y,z} \mathcal{H}_{xyz}$. The three-foliated subsystem symmetries are defined as

$$U_x(g) = \prod_{y=-\infty}^{\infty} \prod_{z=-\infty}^{\infty} u_{xyz}(g),$$

$$U_y(g) = \prod_{x=-\infty}^{\infty} \prod_{z=-\infty}^{\infty} u_{xyz}(g), \quad g \in G_s,$$

$$U_z(g) = \prod_{x=-\infty}^{\infty} \prod_{y=-\infty}^{\infty} u_{xyz}(g). \tag{53}$$

The geometry of the (3+1)D lattice model is illustrated in Fig. 3.

Consider a 3d system with finite extension along all three directions. A third-order SSPT can potentially host nontrivial modes at the corners of the 3d cube. We can view the whole system as a zero-dimensional system with $G_s^{\times 6}$ onsite symmetry. And the symmetry action of $G_s^{\times 6}$ must be anomaly free. The consistency conditions from the anomaly-free requirement give us the classification of the higher-order SSPT states.

Each of the eight corners can at most be a projective representation of the group G_s which are labeled by 2-cocycles $\nu_2^i \in \mathcal{H}^2(G_s, U(1))$ with $i = 1, 2, \ldots, 8$. We will consider the anomaly-free condition for the $G_s^{\times 6}$ symmetry step by step. First, considering the anomaly-free condition for the subsystem symmetry on each individual surface gives us a condition that, on each surface, the four corner projective representations together form a linear representation. In terms of the anomaly action, for instance, on the left yz surface, this

implies

$$S_1[A_1] + S_3[A_1] + S_5[A_1] + S_7[A_1] = 0. \tag{54}$$

Similarly one can write down the other five conditions from the other five surfaces. It is not sufficient to nail down a pattern of the projective representation at the eight corners with these six conditions. However, there is another set of conditions when considering two surfaces with intersections. For example, let us take the left yz surface and the bottom xy surface and turn on the subsystem symmetry gauge field A_1 and A_4. The anomaly-free condition in this case reads

$$S_1[A_1 + A_4] + S_3[A_1 + A_4] + S_5[A_1] + S_7[A_1]$$
$$+ S_2[A_4] + S_4[A_4] = 0. \tag{55}$$

Take a special case where $A_1 = -A_4$, we have

$$S_5[A_1] + S_7[A_1] + S_2[-A_1] + S_4[-A_1] = 0. \tag{56}$$

From Eq. (18), we know that the anomaly action is an even function of the gauge field in the 0+1d case. Therefore we can ignore the sign of the gauge field in the above equation. Combining constraint in Eqs. (54) and (56), the eight response actions have the following relation:

$$S_1[A] = -S_2[A] = S_3[A] = -S_4[A] = S_5[A]$$
$$= -S_6[A] = S_7[A] = -S_8[A] = S[A]. \tag{57}$$

Each of the local degrees of freedom at these corners may carry anomalies of the subsystem symmetry, namely a projective representation of subsystem symmetry G_s classified by $\mathcal{H}^2[G_s, U(1)]$. And the pattern of the projective representations on the eight corners is specified by Eq. (57). Now let us consider the anomaly-free condition for this system. Suppose the background gauge fields of subsystem symmetries on the six surfaces of the cubic systems are $(A_{1,2}, A_{3,4}, A_{5,6})$ as shown in Fig. 3. Let us turn on A_1, A_3, and A_5 (i.e., consider $G_s^{(1)} \times G_s^{(3)} \times G_s^{(5)}$). The total anomaly action should vanish for these three gauge fields, which in this case gives us the following equation:

$$0 = S[A_1] + S[A_3] + S[A_5] - S[A_1 + A_3]$$
$$- S[A_1 + A_5] - S[A_3 + A_5] + S[A_1 + A_3 + A_5]. \tag{58}$$

Equivalently, we can also rephrase the anomaly-free condition in terms of algebraic 2-cocycles: we define an "obstruction" map from $\mathcal{H}^2[G_s, U(1)]$ to $\mathcal{H}^2[G_s^3, U(1)]$, as

$$f(\nu_2)[(g_1, g_1', g_1''), (g_2, g_2', g_2'')]$$
$$= \frac{\nu_2(g_1, g_2)\nu_2(g_1', g_2')\nu_2(g_1'', g_2'')\nu_2(g_1 g_1' g_1'', g_2 g_2' g_2'')}{\nu_2(g_1 g_1', g_2 g_2')\nu_2(g_1 g_1'', g_2 g_2'')\nu_2(g_1' g_1'', g_2' g_2'')}. \tag{59}$$

The anomaly-free condition of the corners [cf. Eq. (58)] requires that the (3+1)D nontrivial SSPT phases with gapless corner modes are labeled by 2-cocycles that will be mapped to a 2-coboundary of the G_s^3 group, $\mathcal{B}^2[G_s^3, U(1)]$, under f-map, otherwise we call the corresponding 2-cocycle is *obstructed*. It is easy to show that considering any other combinations of gauge fields gives us the same condition.

Next, we turn to the case with an additional global symmetry G_g. The anomaly response at a corner (e.g., No. 1) in the presence of both subsystem background gauge field A_s and global background gauge field A_g takes the form of the following:

$$S_1[A_s] + S_1[A_s, A_g]. \tag{60}$$

The first term is the subsystem symmetry anomaly that we have already discussed above. The second term stresses the mixed anomaly of subsystem and global symmetries, hence it can only be nontrivial when both A_s and A_g are nontrivial. From the same anomaly vanishing as before, we find that

$$S_1[A_s, A_g] = -S_2[A_s, A_g] = S_3[A_s, A_g] = -S_4[A_s, A_g]$$
$$= S_5[A_s, A_g] = -S_6[A_s, A_g] = S_7[A_s, A_g]$$
$$= -S_8[A_s, A_g] = S[A_s, A_g] \tag{61}$$

and

$$0 = S[A_{s,1}, A_g] + S[A_{s,3}, A_g] + S[A_{s,5}, A_g]$$
$$- S[A_{s,1} + A_{s,3}, A_g] - S[A_{s,1} + A_{s,5}, A_g]$$
$$- S[A_{s,3} + A_{s,5}, A_g] + S[A_{s,1} + A_{s,3} + A_{s,5}, A_g]. \tag{62}$$

Then we turn into the algebraic cocycle expression that rephrase $S[A_s, A_g]$ as a 2-cocycle ν in $\mathcal{H}^2[G_s \times G_g, U(1)]$. Define the obstruction function f from ν to $\mathcal{H}^2[G_s^3 \times G_g, U(1)]$ as

$$f(\nu)[(g_1, g_1', g_1'', h_1), (g_2, g_2', g_2'', h_2)]$$
$$= \frac{\nu[(g_1, h_1), (g_2, h_2)]\nu[(g_1, h_1), (g_2, h_2)]\nu[(g_1, h_1), (g_2, h_2)]\nu[(g_1 g_1' g_1'', h_1), (g_2 g_2' g_2'', h_2)]}{\nu[(g_1 g_1', h_1), (g_2 g_2', h_2)]\nu[(g_1 g_1'', h_1), (g_2 g_2'', h_2)]\nu[(g_1' g_1'', h_1), (g_2' g_2'', h_2)]}. \tag{63}$$

Here we have denoted the group elements of $G_s^3 \times G_g$ as (g, g', g'', h). The anomaly-free condition is that $f(\nu)$ corresponds to the trivial class in $\mathcal{H}^2[G_s^3 \times G_g, U(1)]$.

B. Microscopic constructions

We now demonstrate that all obstruction-vanishing anomalies can be realized by exact lattice model construction. Consider a (3+1)D lattice model in which each site con-

tains four pairs of projective representations of G_s, each pair includes a projective representation and its inverse (see each green sphere in Fig. 4). A cubic piece that overlaps with eight nearby sites (red cubic in Fig. 4) also includes eight projective representations of subsystem symmetries defined on different plates. An obstruction-free 2-cocycle satisfying the Eq. (59) leads to an anomaly-free red cubic in Fig. 4 automatically, hence we can always introduce some proper interaction to gap out each cubic piece in the
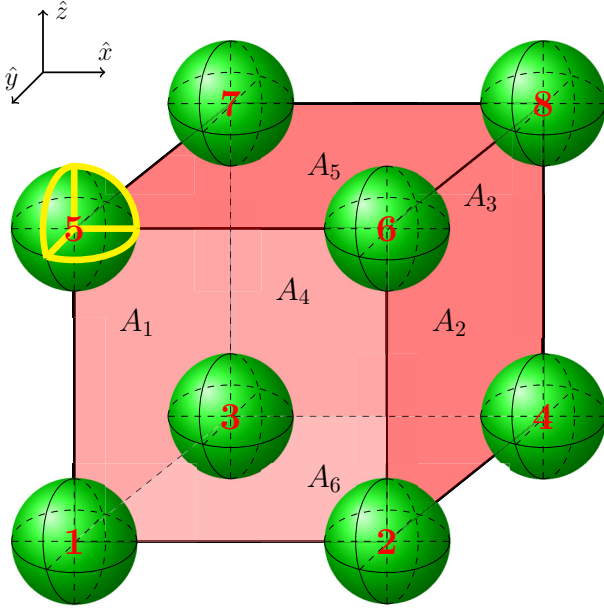
FIG. 4. Lattice model construction of (3+1)D SSPT phases protected by three-foliated codimension-1 subsystem symmetries. Each green sphere depicts a lattice site which is divided into eight equal pieces (the regime enclosed by yellow segments), and there is a projective representation of G_s in each of these pieces. Each red cubic stresses the eight-body interactions in the bulk. A_1, A_2, A_3, A_4, A_5, and A_6 represent the background gauge fields of the subsystem symmetries defined on the left, right, behind, front, top, and bottom surfaces of the red cubic, respectively.

lattice, and a fully gapped bulk has been obtained by our construction.

For each site on the (2+1)D surfaces, there are two pairs of dangling modes that are not included in the bulk cubic interactions, at which we can simply introduce two on-site two-body couplings to cancel their anomalies pairwise, and a fully-gapped surface state has been obtained.

For each site on the (1+1)D hinges, there are three pairs of dangling modes that are not included in the bulk cubic interactions. Similar to the sites on the surface, we can simply introduce three on-site two-body couplings to cancel their anomalies pairwise, and obtain a fully-gapped hinge state.

Finally, for each site at the corners, there are seven dangling modes that are not included in the bulk cubic interactions, at which six of which can be gapped pairwise, similar to the arguments on the hinges. Therefore there is a dangling 0D mode at each corner of the system with OBC, as a projective representation of the subsystem symmetry G_s.

C. Example

In this section, we present a spin model of a (3+1)D nontrivial SSPT phase protected by three-foliated subsystem symmetry $G_s = \mathbb{Z}_2 \times \mathbb{Z}_2$, without global symmetry, by commuting-projector Hamiltonians.

Take the ultraviolet (UV) limit of the truncated operator (53) that is defined in a specific cubic (see Fig. 4), there are eight spin-1/2 degrees of freedom as projective representations of the $\mathbb{Z}_2 \times \mathbb{Z}_2$ group, on each site (green sphere in

Fig. 4), while each red cubic also includes eight spin-1/2 degrees of freedom $\boldsymbol{S}_j$ ($j = 1, \ldots, 8$) from nearby lattice sites. We present the following commuting-projector lattice Hamiltonian:

$$H_x = \sum_{\boldsymbol{R}} \left(S^x_{\boldsymbol{R},1} S^x_{\boldsymbol{R},2} S^x_{\boldsymbol{R},3} S^x_{\boldsymbol{R},4} + S^x_{\boldsymbol{R},1} S^x_{\boldsymbol{R},4} S^x_{\boldsymbol{R},5} S^x_{\boldsymbol{R},8} \right.$$
$$\left. + S^x_{\boldsymbol{R},1} S^x_{\boldsymbol{R},2} S^x_{\boldsymbol{R},5} S^x_{\boldsymbol{R},6} + S^x_{\boldsymbol{R},2} S^x_{\boldsymbol{R},4} S^x_{\boldsymbol{R},5} S^x_{\boldsymbol{R},7} \right), \quad (64)$$

$$H_z = \sum_{\boldsymbol{R}} \left(S^z_{\boldsymbol{R},1} S^z_{\boldsymbol{R},2} S^z_{\boldsymbol{R},3} S^z_{\boldsymbol{R},4} + S^z_{\boldsymbol{R},1} S^z_{\boldsymbol{R},4} S^z_{\boldsymbol{R},5} S^z_{\boldsymbol{R},8} \right.$$
$$\left. + S^z_{\boldsymbol{R},1} S^z_{\boldsymbol{R},2} S^z_{\boldsymbol{R},5} S^z_{\boldsymbol{R},6} + S^z_{\boldsymbol{R},2} S^z_{\boldsymbol{R},4} S^z_{\boldsymbol{R},5} S^z_{\boldsymbol{R},7} \right). \quad (65)$$

It is straightforward to check that the total Hamiltonian $H_x + H_z$ respects the $\mathbb{Z}_2 \times \mathbb{Z}_2$ subsystem symmetry, and provides a nondegenerate ground state. By definition, this spin model will give a dangling spin-1/2 degree of freedom at each corner of the system: for the lattice site on the (2+1)D surface, there are four dangling spin-1/2 degrees of freedom that are not included in the bulk cubic interactions $H_x + H_z$, with on-site $\mathbb{Z}_2 \times \mathbb{Z}_2$ symmetry. We can simply introduce a pair of Heisenberg interaction $\boldsymbol{S} \cdot \boldsymbol{S}'$ on each of these sites to fully gap them out. Similar to the sites on the (1+1)D hinges and corners, there will be a dangling spin-1/2 degree of freedom on each corner of the open system.

On the other hand, a spin-1/2 degree of freedom corresponds to a projective representation of the $\mathbb{Z}_2 \times \mathbb{Z}_2$ group, which is labeled by a 2-cocycle $\nu_2 \in \mathcal{H}^2[\mathbb{Z}_2 \times \mathbb{Z}_2, \mathrm{U}(1)]$, with the following explicit expression:

$$\nu_2(a, b) = (-1)^{a_1 b_2}, \quad (66)$$

where $a = (a_1, a_2)$, $b = (b_1, b_2)$ and $a_{1,2}, b_{1,2} \in \mathbb{Z}_2$. Substitute this explicit form of 2-cocycle into Eq. (59), and we explicitly find that the anomaly-free condition (63) is satisfied automatically. Hence the nontrivial 2-cocycle (66) of $\mathbb{Z}_2 \times \mathbb{Z}_2$ labels a nontrivial third-order SSPT phase protected by three-foliated $\mathbb{Z}_2 \times \mathbb{Z}_2$ subsystem symmetry, which is consistent with above lattice spin model construction.

V. SUMMARY

In this work, we systematically construct and classify interacting fractonic higher-order topological phases in (2+1)D and (3+1)D protected by two-foliated and three-foliated subsystem symmetries and global symmetries.

For two-foliated homogeneous subsystem symmetry G_s and a global symmetry G_g in $(d+1)$D systems, a possible nontrivial SSPT phase is labeled by a d-cocycle $\nu_d \in \mathcal{H}^d[G_s \times G_g, \mathrm{U}(1)]$ satisfying an anomaly free conditions (10) for G_g trivial and (15) for nontrivial global symmetry G_g. We prove that there is no nontrivial two-foliated SSPT phase in (2+1)D systems without a proper global symmetry for Abelian subsystem symmetry G_s. We present several explicit examples of of two-foliated SSPT phases using coupled-wire model constructions. In (2+1)D, we construct a spin model on a square lattice with ring exchange in each plaquette that realizes a higher-order SSPT protected by $G_s = \mathbb{Z}_2$ and $G_g = \mathbb{Z}_2$. In (3+1)D, we first consider a case with $G_s = \mathbb{Z}_2$ and no global symmetry. A wire construction lattice model for a higher-order SSPT using the edge mode of Levin-Gu state is constructed. Subsequently, we consider $G_s = \mathbb{Z}_2$ and

$G_g = \mathbb{Z}_2^{\mathrm{T}}$ and build the coupled-wire model from the Luttinger liquid carrying the mixed anomaly of $\mathbb{Z}_2$ and $\mathbb{Z}_2^{\mathrm{T}}$. Finally, we consider a fermionic example with $G_s = \mathbb{Z}_2^f$ and $G_g = \mathbb{Z}_2$, while the coupled-wire model is constructed from the Luttinger liquid as the edge mode of fermionic Levin-Gu state [74].

For three-foliated homogeneous subsystem symmetry G_s and a global symmetry G_g in (3+1)D systems, a possible nontrivial SSPT phase is labeled by a 2-cocycle in $\mathcal{H}^2[G_s \times G_g, \mathrm{U}(1)]$ satisfying the anomaly-free condition (59). We provide an example of (3+1)D SSPT phase with a spin-1/2 degree of freedom as the concrete third-order topological corner mode, protected by subsystem symmetry $G_s = \mathbb{Z}_2 \times \mathbb{Z}_2$, by exact solvable lattice model construction in Sec. IV C.

Furthermore, in Appendix B and C, we prove that despite the dimensionality of the system with any global symmetry G_g, the inhomogeneous subsystem symmetry will always give a trivial SSPT phase with a layered structure, which will always be trivialized by adhering to lower-dimensional SPT phases protected by subsystem symmetry G_s acting internally, to the surface or hinge of the open boundary of the system.

Our construction and classification of SSPT phases based on the anomaly-free condition are well-defined not only in the bosonic systems but can also be generalized to interacting fermionic systems, and the fermionic higher-order SSPT phases might also be characterized by lower-dimensional group super-cohomological cocycles. Furthermore, with various higher-order SSPT phases, we can investigate the possible fracton phases obtained from the higher-order SSPT phases constructed in this work by gauging the subsystem symmetry [75].

APPENDIX A: COMMENT ON 1-FOLIATED SYSTEMS AND HIGHER-ORDER SSPT

In this section, we comment on one-foliated systems and higher-order SSPT. We argue that there is no nontrivial higher-order SPT phase protected by one-foliated subsystem symmetries even with the help of a global symmetry. In order to achieve a higher-order SSPT phase, we need to have some modes that are anomalous appearing on the corners/hinges. We will argue that, with the one-foliated structure, such anomalous corner modes can be canceled by attaching a lower dimensional SPT on the boundary of the system. We will focus on the case with only subsystem symmetry first.

Let us consider the 2d case. For reference, we can look at Fig. 1. But in the current case, we only have subsystem symmetry along the y direction and no subsystem symmetry along x. In another word, we only have A_1 and A_2 background

gauge fields available. Consider a finite 2d system, if there are nontrivial modes (in this case just projective representations) on the four corners of the system, all of them combined together must be anomaly-free in order to have a well-defined 2d system. Analogous arguments similar to the main text give us anomaly-free conditions where the two projective representations on the left edge must be opposite to each other and the same for the right edge. The crucial difference from the two-foliated case is that there is no subsystem symmetry connecting the left and the right edge, i.e., no additional anomaly-free conditions. Now we can see that we can indeed attach a 1d SPT with G_s symmetry, whose boundary precisely corresponds to the projective representations on the corner, to cancel the corner modes. This is not possible for the two-foliated case because the corner modes carry additional anomalies of the subsystem symmetry from the other foliation direction.

In 3d, the case for third-order SSPT, namely, an SSPT with nontrivial modes at the corners of cubic systems, is very similar to the 2d case we argued above. The same argument for 2d also shows that there is no nontrivial third-order-2 SSPT. We will not elaborate on it here.

In 3d, the case for second-order SSPT is interesting. Suppose we have a one-foliated subsystem symmetry along the z direction, namely in each xy plane there is a symmetry group G_s. Consider a finite cube, there are several possibilities for second-order SSPT. We can have hinge modes along the x or y directions. In this case, the anomaly-free condition is simply that anomalies of the two modes on the same xy plane must cancel each other. With this, we can just attach a 2d G_s SPT on the 2d surface to cancel the hinge mode. Again we emphasize that this attachment is not possible in the two-foliated case because the hinge mode also carries an anomaly of the subsystem symmetry from the orthogonal direction. A more subtle question is whether we can have nontrivial higher-order SSPT where the hinge mode runs along the z direction. We argue that there is no such nontrivial SPT either. Suppose we have four anomalous hinge modes running along z direction on the four hinges of the system. A single hinge mode will carry the anomaly of $G_s^{\times L_z}$ where L_z is the length of z direction. In this case, because each G_s only acts on a single unit cell, the most general anomaly pattern is just given by a series of projective representations of G_s along the chain. In order for the whole system to be anomaly-free, on each xy plane the four projective representations from the four hinges must cancel together. This tells us in each xy plane we can attach 1d SPTs on the four boundaries to cancel all the projective representations on the corners. Again this procedure can be done because we have no additional symmetry constraints from other directions.

Now we consider the effect of the addition of a global symmetry G_g. It is easy to see that, if the corner/hinge modes carry only G_g anomaly, one can always attach a surface G_g SPT to cancel that anomaly without doing any bulk modifications. If the corner/hinge modes carry mixed anomaly of G_s and G_g, one can show that the anomaly-free condition is still the anomalous modes from the same foliation edge/surface cancel together. This in essence means we can attach a lower dimensional SPT on the edge/surface to cancel all the anomalous corners/hinges.

APPENDIX B: INHOMOGENEOUS CASES ARE ALWAYS TRIVIAL

In order to investigate the higher-order SSPT phases, we suppose the symmetry operators only have nontrivial effects at the corner of the regime. Hence the symmetry operator (3) still creates four local excitations at the codimension-2 corners of the regime.

For bosonic systems in $D \leqslant 2$ with unitary symmetry $G_s^x \times G_s^y$, each anomaly class is uniquely determined by the group cohomology class $[\nu] \in \mathcal{H}^{D+2}[G_s^x \times G_s^y, \mathrm{U}(1)]$. This cohomology class can be rephrased by the Künneth formula as

$$\mathcal{H}^{D+2}\big[G_s^x \times G_s^y, \mathrm{U}(1)\big] = \prod_{p=0}^{D+2} \mathcal{H}^{D+2-p}\big(G_s^x, \mathcal{H}^p\big[G_x^y, \mathrm{U}(1)\big]\big),$$

$$(B1)$$

i.e., the first and last term of Eq. (B1) depict the unique anomaly of G_s^x and G_s^y, respectively; all other terms depict the mixed anomaly of G_s^x and G_s^y. The action of anomaly is formally written as

$$S_{\mathrm{anomaly}}^p[A_x, A_y] = \int_{\hat{\mathcal{L}}_y} A_x^* \nu_x^p, \; p = 0, \ldots, D+2, \quad (B2)$$

where A_x is the background gauge field of G_s^x that we view it as a mapping from the space-time manifold M_p as a submanifold of M_{D+2}, to the classifying space BG_s^x, $A_x^* \nu_x^p$ is the pullback of $\mathcal{H}^p(BG_s^x, \mathbb{R}/\mathbb{Z})$, while $\hat{\mathcal{L}}_y$ is the Poincaré dual of the cocycle $\mathcal{L}_y = A_y^* \nu_y^{D+2-p}$ with respect to the space-time M_{D+2}. Physically, $\hat{\mathcal{L}}_y$ stresses the codimension-p domain wall of G_s^y symmetry, and the anomaly action (B2) represents the topological response theory of a p-dimensional G_s^x-SPT phase on the codimension-p domain wall of G_s^y.

For the symmetry operator in Fig. 1, the background gauge fields $A_{1,2,3,4}$ correspond to the symmetry group $(G_s^x \times G_s^y)^2$. Now we turn on the background gauge field A_1 only. Both TL and BL corner theories are coupled to A_1, so the anomaly-free condition implies

$$S_{\mathrm{BL}}[A_1] + S_{\mathrm{TL}}[A_1] = 0. \quad (B3)$$

Similarly, we have

$$\begin{aligned} S_{\mathrm{BR}}[A_2] + S_{\mathrm{TR}}[A_2] &= 0, \\ S_{\mathrm{TL}}[A_3] + S_{\mathrm{TR}}[A_3] &= 0, \\ S_{\mathrm{BL}}[A_4] + S_{\mathrm{BR}}[A_4] &= 0. \end{aligned} \quad (B4)$$

We turn on the background gauge fields A_1 and A_3 (see Fig. 1), and the anomaly carried by the TL corner should be

$$\sum_{p=0}^{d+1} S_{\mathrm{TL}}^p[A_1, A_3] = \sum_{p=0}^{d+1} \int_{\hat{\mathcal{L}}_3} A_1^* \nu_x^p. \quad (B5)$$

The anomaly carried by TR and BL corner are $S_{\mathrm{TR}}[A_3]$ and $S_{\mathrm{BL}}[A_1]$, respectively. We notice that only the TL corner carries the mixed anomaly of A_1 and A_3 [$p \neq 0$ in Eq. (B5)], hence the anomaly-free condition requires that all mixed anomalies at the TL corner vanish. Equivalently, the anomaly carried by a corner (B2) should reduce to the sum of a unique

anomaly of vertical and horizontal subsystem symmetries as

$$S_{\mathrm{anomaly}}[A_x, A_y] = S_{\mathrm{anomaly}}[A_x] + S_{\mathrm{anomaly}}[A_y]. \quad (B6)$$

Hence the anomaly-free conditions are exactly highlighted in Eqs. (B3) and (B4) and all mixed anomalies of subsystem symmetries should vanish.

Then we consider a codimension-1 SPT phase protected by G_s^y on the system's left edge, with the enlarged truncated symmetry operator applying to the whole system. This SPT phase leaves codimension-2 modes at the TL and BL corners, carrying the anomalies of the background gauge field A_1 phrased by the actions $S_{\mathrm{BL}}'[A_1]$ and $S_{\mathrm{TL}}'[A_1]$, satisfying

$$S_{\mathrm{BL}}'[A_1] + S_{\mathrm{TL}}'[A_1] = 0. \quad (B7)$$

We simply choose $S_{\mathrm{BL}}'[A_1] = -S_{\mathrm{BL}}[A_1]$ and $S_{\mathrm{TL}}'[A_1] = -S_{\mathrm{TL}}[A_1]$, and the bulk anomaly of the background gauge field A_1 is canceled by this codimension-1 SPT phase on the left boundary. Similarly, the bulk anomaly of the background gauge field A_3 can be canceled by an additional codimension-1 SPT phase protected by G_s^x symmetry on the top boundary. As a consequence, there is no higher-order SSPT phase for two-foliated inhomogeneous subsystem symmetry.

APPENDIX C: INHOMOGENEOUS SUBSYSTEM SYMMETRIES IN 3D

For inhomogeneous subsystem symmetries, there are several possible scenarios.

(1) The subsystem symmetries in all three directions act respectively that can be different. We denote the subsystem symmetries defined in yz, xz, and xy planes as G_x, G_y and G_z, respectively.

(2) The subsystem symmetries in two of three directions act identically, and the other subsystem symmetry acts separately. We denote these subsystem symmetries by two groups G_s^1 and G_s^2, respectively.

For the first scenario, the three-foliated subsystem symmetries should be redefined as

$$\begin{aligned} U_x(g_x) &= \prod_{y=-\infty}^{\infty} \prod_{z=-\infty}^{\infty} u_{xyz}^x(g_x) \\ U_y(g_y) &= \prod_{x=-\infty}^{\infty} \prod_{z=-\infty}^{\infty} u_{xyz}^y(g_y), \quad \begin{cases} g_x \in G_x \\ g_y \in G_y, \\ g_z \in G_z \end{cases} \quad (C1) \\ U_z(g_z) &= \prod_{x=-\infty}^{\infty} \prod_{y=-\infty}^{\infty} u_{xyz}^z(g_z) \end{aligned}$$

where $(u_{xyz}^x(g_x), u_{xyz}^y(g_y), u_{xyz}^z(g_z))$ are linear representations of the groups (G_x, G_y, G_z), respectively. The local degrees of freedom at the corners should be labeled by the projective representations of $G_x \times G_y \times G_z$ group, classified by $\mathcal{H}^2[G_x \times G_y \times G_z, \mathrm{U}(1)]$. The action of anomaly is formally written as

$$S_{\mathrm{anomaly}}^p[A_i, A_j] = \int_{\hat{\mathcal{L}}_j} A_i^* \nu_i^p, \; p = 0, 1, 2, \quad (C2)$$

where A_i and A_j are background gauge fields of G_s^i and G_s^j ($i, j = x, y, z$ and $i \neq j$) that we view them as maps from the space-time manifolds M_p and M_{2-p} as the submanifolds of

M_2 to the classifying spaces BG_s^i and BG_s^j, and $A_{i,j}^* \nu_{i,j}^p$ is the pullback of $\mathcal{H}^p(BG_s^{i,j}, \mathbb{R}/\mathbb{Z})$, while $\hat{\mathcal{L}}_j$ is the Poincaré dual of the cocycle $\mathcal{L}_j = A_j^* \nu_j^{2-p}$ with respect to the space-time M_2.

For the truncated symmetry operator in Fig. 3, the background gauge fields A_j $(j = 1, \dots, 6)$ correspond to the symmetry group $(G_s^x \times G_s^y \times G_s^z)^2$. We first turn on the background gauge field A_1 only, the anomaly-free condition implies the following constraints on the anomaly action as

$$S_1[A_1] + S_3[A_1] + S_5[A_1] + S_7[A_1] = 0 \qquad \text{(C3)}$$

and other five similar constraints from the other five surfaces.

Then we turn on the background gauge fields A_1 and A_4, and the total anomaly carried by the corner-1/-4 is phrased by the following action:

$$\sum_{p=0}^{2} S_j^p[A_1, A_4] = \sum_{p=0}^{2} \int_{\hat{\mathcal{L}}_4} A_1^* \nu_x^p, \ j = 1, 4. \qquad \text{(C4)}$$

The mixed anomalies carried by corner-1 and corner-4 satisfy the following constraint to ensure the anomaly-free condition as

$$S_1^1[A_1, A_4] = -S_4^1[A_1, A_4] \qquad \text{(C5)}$$

and similar for all other mixed anomalies. Therefore we always have some way to find an anomaly-free bulk lattice model.

Then we consider the possible trivializations of the constructed model of three-foliated inhomogeneous SSPT phases. For the corner mode carrying a unique anomaly of the subsystem symmetry along a specific direction, for instance, in yz plane with background gauge field A_1, which is labeled by a 2-cocycle $\nu_2 \in \mathcal{H}^2[G_x, \mathrm{U}(1)]$ at the corner-7, consider the $(1+1)$D hinge of left and behind surfaces, at which the subsystem symmetries G_x and G_y act as global symmetries. Consider a $(1+1)$D SPT phase protected by G_x symmetry while G_y and G_z act on it trivially, we choose $-\nu_2 \in \mathcal{H}^2[G_x, \mathrm{U}(1)]$ to characterize this $(1+1)$D SPT phase, whose dangling edge mode at corner-7 will annihilate the dangling gapless mode from bulk lattice model construction, i.e., the corresponding bulk state is *trivialized*. Similar to G_y and G_z, all corner modes carrying the unique anomaly of $G_{x,y,z}$ can be trivialized by adhering a $(1+1)$D SPT phase to the hinge of the cubic.

For the corner mode carrying a mixed anomaly of the subsystem symmetries along two directions. Without loss of generality, we consider the $(0+1)$D dangling mode carrying the mixed anomaly of G_x and G_y, characterized by a cup product of two 1-cocycles:

$$\nu_1^x(g_x) \cup \nu_1^y(g_y), \ \begin{cases} \nu_1^x(g_x) \in \mathcal{H}^1[G_x, \mathrm{U}(1)] \\ \nu_1^y(g_y) \in \mathcal{H}^1[G_y, \mathrm{U}(1)] \end{cases}. \qquad \text{(C6)}$$

Repeatedly consider the $(1+1)$D hinge of left and behind surfaces, at which G_x and G_y act as global symmetries. Consider a $(1+1)$D SPT phase protected by $G_x \times G_y$ while G_z acts on it trivially, we choose $-\nu_1^x \cup \nu_1^y \in \mathcal{H}^1[G_x, \mathcal{H}^1[G_y, \mathrm{U}(1)]]$ to characterize this $(1+1)$D SPT phase, whose dangling edge mode at corner-7 will annihilate the dangling gapless mode from bulk lattice model construction, i.e., the corresponding bulk state is also trivialized. Similar for all other mixed anomalies carried by corner modes.

We conclude that for the scenario of which the subsystem symmetries in all three directions act respectively, the classification of third-order SSPT phases should be trivial because all possible bulk lattice model constructions are trivialized by adhering a $(1+1)$D SPT phase to the hinges of the system.

For the second scenario that the subsystem symmetries in two of three directions act identically, while the subsystem symmetry in the other direction act separately, the three-foliated subsystem symmetries should be redefined as (without loss of generality, we suppose the subsystem symmetry on the xz and yz planes is G_s^1, while the subsystem symmetry on the xy plane is G_s^2):

$$U_x(g_1) = \prod_{y=-\infty}^{\infty} \prod_{z=-\infty}^{\infty} u_{xyz}^1(g_1)$$

$$U_y(g_1) = \prod_{x=-\infty}^{\infty} \prod_{z=-\infty}^{\infty} u_{xyz}^1(g_1), \ \begin{cases} g_1 \in G_s^1 \\ g_2 \in G_s^2 \end{cases}, \qquad \text{(C7)}$$

$$U_z(g_2) = \prod_{x=-\infty}^{\infty} \prod_{y=-\infty}^{\infty} u_{xyz}^2(g_2)$$

where $u_{xyz}^1(g_1)$ and $u_{xyz}^2(g_2)$ are linear representations of the groups G_s^1 and G_s^2, respectively. The local degrees of freedom at the corners are projective representations of the group $G_s^1 \times G_s^2$, classified by

$$\mathcal{H}^2[G_s^1 \times G_s^2, \mathrm{U}(1)] = \mathcal{H}^2[G_s^1, \mathrm{U}(1)],$$
$$\times \mathcal{H}^2[G_s^2, \mathrm{U}(1)] \times \mathcal{H}^1[G_s^1, \mathcal{H}^1[G_s^2, \mathrm{U}(1)]], \qquad \text{(C8)}$$

in terms of background gauge fields, the action of the anomaly of $G_s^1 \times G_s^2$ is formally written as

$$S_{\text{anomaly}}^p[A_{1,s}, A_{2,s}] = \int_{\hat{\mathcal{L}}_2} A_{1,s}^* \nu_1^p, \ p = 0, 1, 2, \qquad \text{(C9)}$$

where A_1 and A_2 are background gauge fields of G_s^1 and G_s^2 that we view as maps from the space-time manifolds M_p and M_{2-p} as the submanifolds of M_2 to the classifying spaces BG_s^1 and BG_s^2, respectively; $A_{j,s}^* \nu_j^p$ $(j = 1, 2)$ is the pullback of $\mathcal{H}^p(BG_s^j, \mathbb{R}/\mathbb{Z})$, while $\hat{\mathcal{L}}_2$ is the Poincaré dual of the cocycle $\mathcal{L}_2 = A_{2,s}^* \nu_2^{2-p}$ with respect to the space-time M_2.

Following the similar arguments with above $G_s^x \times G_s^y \times G_s^z$ cases, we conclude that we can always find some fully gapped, anomaly-free bulk lattice model. Then we focus on some possible trivializations by sticking some lower-dimensional SPT phases on the edge/hinge.

Firstly, for corner-7 carrying a projective representation $\nu_2^2 \in \mathcal{H}^2[G_s^2, \mathrm{U}(1)]$, we focus on the hinge of the top and behind surfaces at which the subsystem symmetry G_s^2 acts as a global symmetry: Consider a $(1+1)$D SPT phase protected by G_s^2 adhered to this hinge, while the subsystem symmetry G_s^1 acts on this $(1+1)$D SPT state trivially. We choose $-\nu_2^2 \in \mathcal{H}^2[G_s^2, \mathrm{U}(1)]$ to characterize this adhered $(1+1)$D SPT phase, whose dangling edge mode at the corner-7 will annihilate the dangling gapless mode from bulk lattice model construction, i.e., the corresponding bulk state is *trivialized*.

Subsequently, for corner-7 carrying a projective representation $\nu_2^1 \in \mathcal{H}^2[G_s^1, \mathrm{U}(1)]$, we focus on the hinge of the left and behind surfaces at which the subsystem symmetry G_s^1

acts as a global symmetry: Consider a (1+1)D SPT phase protected by G_s^1 adhered to this hinge, while the subsystem symmetry G_s^2 acts on this (1+1)D SPT state trivially. We choose $-\nu_2^1 \in \mathcal{H}^2[G_s^1, U(1)]$ to characterize this adhered (1+1)D SPT phase, whose dangling edge mode at the corner-7 will annihilate the dangling gapless mode from bulk lattice model construction, i.e., the corresponding bulk state is *trivialized*.

Finally, for corner-7 carrying a projective representation with the mixed anomaly of G_s^1 and G_s^2, we repeatedly focus on the hinge of the top and behind surfaces at which the subsystem symmetries defined on the xy plane and xz plane act as global symmetries: consider a (1+1)D SPT phase protected by $G_s^1 \times G_s^2$ (from the subsystem symmetries defined on the xy and xz planes) adhered to this hinge, while the subsystem symmetry defined on the yz plane acts on this (1+1)D SPT state trivially. We choose $-\nu_1^1 \cup \nu_1^2 \in \mathcal{H}^1[G_s^1, \mathcal{H}^1[G_s^2, U(1)]]$ to characterize this adhered (1+1)D SPT phase, whose dangling edge mode at the corner-7 will annihilate the dangling gapless mode from bulk lattice model construction, i.e., the corresponding bulk state is also *trivialized*.

Now we have rigorously proved that for three-foliated inhomogeneous subsystem symmetries in (3+1)D systems, there is no nontrivial SSPT phase with a third-order topological corner state.

[1] Z.-C. Gu and X.-G. Wen, Tensor-entanglement-filtering renormalization approach and symmetry-protected topological order, Phys. Rev. B **80**, 155131 (2009).

[2] X. Chen, Z.-C. Gu, Z.-X. Liu, and X.-G. Wen, Symmetry-protected topological orders in interacting bosonic systems, Science **338**, 1604 (2012).

[3] X. Chen, Z.-C. Gu, Z.-X. Liu, and X.-G. Wen, Symmetry protected topological orders and the group cohomology of their symmetry group, Phys. Rev. B **87**, 155114 (2013).

[4] T. Senthil, Symmetry-protected topological phases of quantum matter, Annu. Rev. Condens. Matter Phys. **6**, 299 (2015).

[5] Y.-M. Lu and A. Vishwanath, Theory and classification of interacting integer topological phases in two dimensions: A chern-simons approach, Phys. Rev. B **86**, 125119 (2012).

[6] D. S. Freed, Short-range entanglement and invertible field theories, arXiv:1406.7278 [cond-mat.str-el].

[7] D. S. Freed and M. J. Hopkins, Reflection positivity and invertible topological phases, Geom. Topol. **25**, 1165 (2021).

[8] Z.-C. Gu and X.-G. Wen, Symmetry-protected topological orders for interacting fermions: Fermionic topological nonlinear σ models and a special group supercohomology theory, Phys. Rev. B **90**, 115141 (2014).

[9] Q.-R. Wang and Z.-C. Gu, Towards a Complete Classification of Symmetry-Protected Topological Phases for Interacting Fermions in Three Dimensions and a General Group Supercohomology Theory, Phys. Rev. X **8**, 011055 (2018).

[10] Q.-R. Wang and Z.-C. Gu, Construction and Classification of Symmetry-Protected Topological Phases in Interacting Fermion Systems, Phys. Rev. X **10**, 031055 (2020)..

[11] A. Kapustin, Symmetry protected topological phases, anomalies, and cobordisms: Beyond group cohomology, arXiv:1403.1467 [cond-mat.str-el].

[12] A. Kapustin, R. Thorngren, A. Turzillo, and Z. Wang, Fermionic symmetry protected topological phases and cobordisms, J. High Energy Phys. 12 (2015) 052.

[13] A. Kapustin and R. Thorngren, Fermionic spt phases in higher dimensions and bosonization, J. High Energy Phys. 10 (2017) 080.

[14] C. Wang, C.-H. Lin, and Z.-C. Gu, Interacting fermionic symmetry-protected topological phases in two dimensions, Phys. Rev. B **95**, 195147 (2017).

[15] M. Cheng, Z. Bi, Y.-Z. You, and Z.-C. Gu, Classification of symmetry-protected phases for interacting fermions in two dimensions, Phys. Rev. B **97**, 205109 (2018).

[16] F. Schindler, A. M. Cook, M. G. Vergniory, Z. Wang, S. S. P. Parkin, B. A. Bernevig, and T. Neupert, Higher-order topological insulators, Sci. Adv. **4**, eaat0346 (2018).

[17] W. A. Benalcazar, B. A. Bernevig, and T. L. Hughes, Quantized electric multipole insulators, Science **357**, 61 (2017).

[18] W. A. Benalcazar, B. A. Bernevig, and T. L. Hughes, Electric multipole moments, topological multipole moment pumping, and chiral hinge states in crystalline insulators, Phys. Rev. B **96**, 245115 (2017).

[19] F. Zhang, C. L. Kane, and E. J. Mele, Surface State Magnetization and Chiral Edge States on Topological Insulators, Phys. Rev. Lett. **110**, 046404 (2013).

[20] R.-X. Zhang, W. S. Cole, X. Wu, and S. Das Sarma, Higher-Order Topology and Nodal Topological Superconductivity in Fe(Se,Te) Heterostructures, Phys. Rev. Lett. **123**, 167001 (2019).

[21] L. Fu, Topological Crystalline Insulators, Phys. Rev. Lett. **106**, 106802 (2011).

[22] T. H. Hsieh, H. Lin, J. Liu, W. Duan, A. Bansil, and L. Fu, Topological crystalline insulators in the snte material class, Nat. Commun. **3**, 982 (2012).

[23] H. Isobe and L. Fu, Theory of interacting topological crystalline insulators, Phys. Rev. B **92**, 081304(R) (2015).

[24] H. Song, S.-J. Huang, L. Fu, and M. Hermele, Topological Phases Protected by Point Group Symmetry, Phys. Rev. X **7**, 011020 (2017).

[25] S.-J. Huang, H. Song, Y.-P. Huang, and M. Hermele, Building crystalline topological phases from lower-dimensional states, Phys. Rev. B **96**, 205106 (2017).

[26] R. Thorngren and D. V. Else, Gauging Spatial Symmetries and the Classification of Topological Crystalline Phases, Phys. Rev. X **8**, 011040 (2018).

[27] F. Tang, H. C. Po, A. Vishwanath, and X. Wan, Comprehensive search for topological materials using symmetry indicators, Nature (London) **566**, 486 (2019).

[28] N. Bultinck, B. A. Bernevig, and M. P. Zaletel, Three-dimensional superconductors with hybrid higher-order topology, Phys. Rev. B **99**, 125149 (2019).

[29] B. Roy, Higher-order topological superconductors in $\mathscr{P}$-, $\mathscr{T}$-odd quadrupolar dirac materials, Phys. Rev. B **101**, 220506(R) (2020).

[30] B. Roy and V. Juričić, Mixed-parity octupolar pairing and corner majorana modes in three dimensions, Phys. Rev. B **104**, L180503 (2021).

[31] K. Laubscher, D. Loss, and J. Klinovaja, Fractional topological superconductivity and parafermion corner states, Phys. Rev. Res. **1**, 032017(R) (2019).

[32] K. Laubscher, D. Loss, and J. Klinovaja, Majorana and parafermion corner states from two coupled sheets of bilayer graphene, Phys. Rev. Res. **2**, 013330 (2020).

[33] J.-H. Zhang, Strongly correlated crystalline higher-order topological phases in two-dimensional systems: A coupled-wire study, Phys. Rev. B **106**, L020503 (2022).

[34] Y. Tanaka, Z. Ren, T. Sato, K. Nakayama, S. Souma, T. Takahashi, K. Segawa, and Y. Ando, Experimental realization of a topological crystalline insulator in snte, Nat. Phys. **8**, 800 (2012).

[35] P. Dziawa, B. J. Kowalski, K. Dybko, R. Buczko, A. Szczerbakow, M. Szot, E. Łusakowska, T. Balasubramanian, B. M. Wojek, M. H. Berntsen, O. Tjernberg, and T. Story, Topological crystalline insulator states in $Pb_{1-x}Sn_xSe$, Nat. Mater. **11**, 1023 (2012).

[36] Y. Okada, M. Serbyn, H. Lin, D. Walkup, W. Zhou, C. Dhital, M. Neupane, S. Xu, Y. J. Wang, R. Sankar, F. Chou, A. Bansil, M. Z. Hasan, S. D. Wilson, L. Fu, and V. Madhavan, Observation of dirac node formation and mass acquisition in a topological crystalline insulator, Science **341**, 1496 (2013).

[37] J. Ma, C. Yi, B. Lv, Z. Wang, S. Nie, L. Wang, L. Kong, Y. Huang, P. Richard, P. Zhang, K. Yaji, K. Kurado, S. Shin, H. Weng, B. A. Bernevig, Y. Shi, T. Qian, and H. Ding, Experimental evidence of hourglass fermion in the candidate nonsymmorphic topological insulator khgsb, Sci. Adv. **3**, e1602415 (2017).

[38] Z. Song, S.-J. Huang, Y. Qi, C. Fang, and M. Hermele, Topological states from topological crystals, Sci. Adv. **5**, eaax2007 (2019).

[39] Z. Song, C. Fang, and Y. Qi, Real-space recipes for general topological crystalline states, Nat. Commun. **11**, 4197 (2020)..

[40] M. Cheng and C. Wang, Rotation symmetry-protected topological phases of fermions, Phys. Rev. B **105**, 195154 (2022).

[41] J.-H. Zhang, Q.-R. Wang, S. Yang, Y. Qi, and Z.-C. Gu, Construction and classification of point-group symmetry-protected topological phases in two-dimensional interacting fermionic systems, Phys. Rev. B **101**, 100501(R) (2020).

[42] J.-H. Zhang, S. Yang, Y. Qi, and Z.-C. Gu, Real-space construction of crystalline topological superconductors and insulators in 2d interacting fermionic systems, Phys. Rev. Research **4**, 033081 (2022).

[43] J.-H. Zhang, Y. Qi, and Z.-C. Gu, Construction and classification of crystalline topological superconductor and insulators in three-dimensional interacting fermion systems, (2022), arXiv:2204.13558 [cond-mat.str-el].

[44] S. Vijay, J. Haah, and L. Fu, Fracton topological order, generalized lattice gauge theory, and duality, Phys. Rev. B **94**, 235157 (2016).

[45] R. M. Nandkishore and M. Hermele, Fractons, Annu. Rev. Condens. Matter Phys. **10**, 295 (2019).

[46] M. Pretko, X. Chen, and Y. You, Fracton phases of matter, Int. J. Mod. Phys. A **35**, 2030003 (2020).

[47] S. Pai and M. Hermele, Fracton fusion and statistics, Phys. Rev. B **100**, 195136 (2019).

[48] P. Wang, G. Yu, Y. H. Kwan, Y. Jia, S. Lei, S. Klemenz, F. A. Cevallos, R. Singha, T. Devakul, K. Watanabe, T. Taniguchi, S. L. Sondhi, R. J. Cava, L. M. Schoop, S. A. Parameswaran, and S. Wu, One-dimensional luttinger liquids in a two-dimensional moirélattice, Nature (London) **605**, 57 (2022).

[49] L. Ye, S. Fang, M. G. Kang, J. Kaufmann, Y. Lee, J. Denlinger, C. Jozwiak, A. Bostwick, E. Rotenberg, E. Kaxiras, D. C. Bell, O. Janson, R. Comin, and J. G. Checkelsky, A flat band-induced correlated kagome metal, (2021), arXiv:2106.10824 [cond-mat.mtrl-sci].

[50] L. Zou and T. Senthil, Dimensional decoupling at continuous quantum critical mott transitions, Phys. Rev. B **94**, 115113 (2016).

[51] Y. You, T. Devakul, F. J. Burnell, and S. L. Sondhi, Subsystem symmetry protected topological order, Phys. Rev. B **98**, 035112 (2018).

[52] T. Devakul, Y. You, F. J. Burnell, and S. Sondhi, Fractal symmetric phases of matter, SciPost Phys. **6**, 007 (2019).

[53] T. Devakul, D. J. Williamson, and Y. You, Classification of subsystem symmetry-protected topological phases, Phys. Rev. B **98**, 235121 (2018).

[54] T. Devakul, W. Shirley, and J. Wang, Strong planar subsystem symmetry-protected phases and their dual fracton orders, Phys. Rev. Res. **2**, 012059(R) (2020).

[55] D. J. Williamson, Z. Bi, and M. Cheng, Fractonic matter in symmetry-enriched $u(1)$ gauge theory, Phys. Rev. B **100**, 125150 (2019).

[56] J. May-Mann and T. L. Hughes, Corner modes and ground-state degeneracy in models with gaugelike subsystem symmetries, Phys. Rev. B **100**, 165108 (2019).

[57] Y. You, T. Devakul, F. J. Burnell, and S. L. Sondhi, Symmetric fracton matter: Twisted and enriched, Ann. Phys. **416**, 168140 (2020).

[58] D. T. Stephen, J. Garre-Rubio, A. Dua, and D. J. Williamson, Subsystem symmetry enriched topological order in three dimensions, Phys. Rev. Res. **2**, 033331 (2020).

[59] J. May-Mann and T. L. Hughes, Topological dipole conserving insulators and multipolar responses, Phys. Rev. B **104**, 085136 (2021).

[60] N. Tantivasadakarn and S. Vijay, Searching for fracton orders via symmetry defect condensation, Phys. Rev. B **101**, 165143 (2020).

[61] N. Tantivasadakarn, Jordan-wigner dualities for translation-invariant hamiltonians in any dimension: Emergent fermions in fracton topological order, Phys. Rev. Res. **2**, 023353 (2020).

[62] N. Tantivasadakarn, W. Ji, and S. Vijay, Hybrid fracton phases: Parent orders for liquid and nonliquid quantum phases, Phys. Rev. B **103**, 245136 (2021).

[63] N. Tantivasadakarn, W. Ji, and S. Vijay, Non-abelian hybrid fracton orders, Phys. Rev. B **104**, 115117 (2021).

[64] Y. You, J. Bibo, F. Pollmann, and T. L. Hughes, Fracton critical point in higher-order topological phase transition, (2020), arXiv:2008.01746.

[65] Y. You, F. J. Burnell, and T. L. Hughes, Multipolar topological field theories: Bridging higher order topological insulators and fractons, Phys. Rev. B **103**, 245128 (2021).

[66] Y. You, J. Bibo, T. L. Hughes, and F. Pollmann, Fractonic critical point proximate to a higher-order topological insulator: How does uv blend with ir?, arXiv:2101.01724.

[67] J. May-Mann, Y. You, T. L. Hughes, and Z. Bi, Interaction-enabled fractonic higher-order topological phases, Phys. Rev. B **105**, 245122 (2022).

[68] J. C. Y. Teo and C. L. Kane, From luttinger liquid to non-abelian quantum hall states, Phys. Rev. B **89**, 085101 (2014).

[69] J. Wang and X.-G. Wen, Non-perturbative regularization of 1+1d anomaly-free chiral fermions and bosons: On the equivalence of anomaly matching conditions and boundary gapping rules, Phys. Rev. B **107**, 014311 (2023).

[70] M. Levin and Z.-C. Gu, Braiding statistics approach to symmetry-protected topological phases, Phys. Rev. B **86**, 115109 (2012).

[71] F. D. M. Haldane, Stability of Chiral Luttinger Liquids and Abelian Quantum Hall States, Phys. Rev. Lett. **74**, 2090 (1995).

[72] S.-Q. Ning, C. Wang, Q.-R. Wang, and Z.-C. Gu, Edge theories of two-dimensional fermionic symmetry protected topological phases protected by unitary abelian symmetries, Phys. Rev. B **104**, 075151 (2021).

[73] C. Heinrich and M. Levin, Criteria for protected edge modes with $\mathbb{z}_2$ symmetry, Phys. Rev. B **98**, 035101 (2018).

[74] Z.-C. Gu and M. Levin, Effect of interactions on two-dimensional fermionic symmetry-protected topological phases with z_2 symmetry, Phys. Rev. B **89**, 201113(R) (2014).

[75] W. Shirley, K. Slagle, and X. Chen, Foliated fracton order from gauging subsystem symmetries, SciPost Phys. **6**, 041 (2019).